Check for updates

NEURODEGENERATION

Copyright © 2025 The Authors, some rights reserved; exclusive licensee American Association for the Advancement of Science. No claim to original U.S. Government Works

Proteomic analysis reveals distinct cerebrospinal fluid signatures across genetic frontotemporal dementia subtypes

Aitana Sogorb-Esteve[1,2]*†, Sophia Weiner[3]†, Joel Simrén[3]†, Imogen J. Swift[1,2], Martina Bocchetta[2,4], Emily G. Todd[2], David M. Cash[1,2], Arabella Bouzigues[2], Lucy L. Russell[2], Phoebe H. Foster[2], Eve Ferry-Bolder[2], John C. van Swieten[5], Lize C. Jiskoot[5], Harro Seelaar[5], Raquel Sanchez-Valle[6], Robert Laforce[7], Caroline Graff[8,9], Daniela Galimberti[10,11], Rik Vandenberghe[12,13,14], Alexandre de Mendonça[15], Pietro Tiraboschi[16], Isabel Santana[17,18], Alexander Gerhard[19,20], Johannes Levin[21,22,23], Sandro Sorbi[24,25], Markus Otto[26,27], Florence Pasquier[28,29,30], Simon Ducharme[31,32], Chris R. Butler[33,34], Isabelle Le Ber[35,36,37], Elizabeth Finger[38], Maria Carmela Tartaglia[39], Mario Masellis[40], James B. Rowe[41], Matthis Synofzik[42,43], Fermin Moreno[44,45], Barbara Borroni[46,47], GENFI‡, Kaj Blennow[3,48,49,50], Henrik Zetterberg[1,3,48,51,52,53]†, Jonathan D. Rohrer[2]†, Johan Gobom[3,48]†

We used an untargeted mass spectrometric approach, tandem mass tag proteomics, for the identification of proteomic signatures in genetic frontotemporal dementia (FTD). A total of 238 cerebrospinal fluid (CSF) samples from the Genetic FTD Initiative were analyzed, including samples from 107 presymptomatic (44 *C9orf72*, 38 *GRN*, and 25 *MAPT*) and 55 symptomatic (27 *C9orf72*, 17 *GRN*, and 11 *MAPT*) mutation carriers as well as 76 mutation-negative controls ("noncarriers"). We found shared and distinct proteomic alterations in each genetic form of FTD. Among the proteins significantly altered in symptomatic mutation carriers compared with noncarriers, we found that a set of proteins including neuronal pentraxin 2 and fatty acid binding protein 3 changed across all three genetic forms of FTD and patients with Alzheimer's disease from previously published datasets. We observed differential changes in lysosomal proteins among symptomatic mutation carriers with marked abundance decreases in *MAPT* carriers but not other carriers. Further, we identified mutation-associated proteomic changes already evident in presymptomatic mutation carriers. Weighted gene coexpression network analysis combined with gene ontology annotation revealed clusters of proteins enriched in neurodegeneration and glial responses as well as synapse- or lysosome-related proteins indicating that these are the central biological processes affected in genetic FTD. These clusters correlated with measures of disease severity and were associated with cognitive decline. This study revealed distinct proteomic changes in the CSF of patients with genetic FTD, providing insights into the pathological processes involved in the disease. In addition, we identified proteins that warrant further exploration as diagnostic and prognostic biomarker candidates.

INTRODUCTION

Frontotemporal dementia (FTD) is an umbrella term referring to a group of progressive neurodegenerative disorders, which typically present with behavioral changes {behavioral variant, language problems (primary progressive aphasia), or motor impairment [either FTD with amyotrophic lateral sclerosis (ALS) or FTD with parkinsonism]} (*1*). Although less common than Alzheimer's disease (AD), dementia with Lewy bodies, and vascular dementia, FTD is a leading cause of early onset dementia (*2*). The underlying molecular basis of FTD is complex, but most cases can be attributed to a frontotemporal lobar degeneration (FTLD) pathology, with cellular inclusions of tau, TAR DNA binding protein 43 (TDP-43), or FET proteins [FUS (fused in sarcoma), EWS (Ewing sarcoma), and TAF15 (TATA-binding associated factor 15)] (*3*). Unlike AD, around a third of FTD cases have a genetic cause, with the most common mutations occurring in three genes: *GRN* (progranulin) and *C9orf72* (chromosome 9 open reading frame 72), both of which are typically accompanied by an underlying TDP-43 proteinopathy, and *MAPT* (microtubule-associated protein tau), manifesting as tauopathy (*1*, *4*).

In FTD, the complex relationship between clinical presentations and underlying molecular pathology poses a challenge for its diagnosis and treatment. AD can be viewed as a successful example of how the introduction of cerebrospinal fluid (CSF) biomarker–assisted diagnosis has led to recent therapeutic advances (*5*) with the potential to revolutionize its treatment. In the case of FTD, however, the historic lack of biomarkers, as well as the complex relationship between clinical symptomatology and underlying pathophysiology, have so far hampered such advancements. Nonetheless, there are biomarkers that show promise also in the context of FTD. Neurofilament light chain (NfL) has emerged as a promising, although disease-nonspecific, biomarker in differentiating FTD from primary psychiatric causes of behavioral symptoms (*6*) and, because plasma NfL increases in concentration in the presymptomatic phase of genetic FTD, also as a biomarker to detect neurodegeneration onset and disease intensity (*7*). Although there are indications that group-level concentrations of NfL are highest (at least in plasma) in *GRN* carriers (*8*), NfL cannot be used to identify the underlying pathology. For this purpose, mutation- or pathology-specific biomarkers are needed, with current examples being limited, such as low plasma/CSF progranulin as an indication of an underlying *GRN* mutation resulting in haploinsufficiency (*9*, *10*), or promising new results on TDP-43 or 3R/4R tau protein in plasma-derived extracellular vesicles (*11*) need further replication. Because of

Downloaded from https://www.science.org at Universita Degli Studi Di Trento on February 10, 2025

the lack of an antemortem gold standard for FTLD-tau and TDP-43 pathologies, sporadic FTD is likely not an ideal model to develop previously unidentified biomarkers at present. In familial FTD, however, the relationship between genetic mutation and resulting pathology may provide a context that allows the identification of such markers.

Previous studies using antibody-based methods (*12*–*14*) or mass spectrometric techniques (*15*, *16*) have identified several FTD biomarker candidates, including NfL, neurofilament medium (NfM) and heavy (NfH), neuronal pentraxins, chitinase-3–like protein 1 (CHI3L1, also known as YKL-40), and ubiquitin carboxy-terminal hydrolase L1 (UCHL1). However, none of these proteins have proven specific for either FTLD or its subtypes, with similar alterations being seen in other neurodegenerative disorders, such as AD, Creutzfeldt-Jakob disease, or ALS (*14*, *17*–*21*).

In this study, we adopted an untargeted proteomics approach, using high-resolution mass spectrometry (MS) combined with tandem mass tag (TMT), to measure CSF proteins in a large, well-characterized genetic FTD cohort: the Genetic FTD Initiative (GENFI) study. We aimed to measure changes in low-abundance proteins not previously implicated in FTD to identify proteomic signatures of symptomatic groups carrying the most common genetic mutations causing FTD and therefore potentially distinguish specific underlying pathologies. Furthermore, we explored CSF proteomic changes that may identify mutation carriers at the presymptomatic stage of the disease, as has been done previously in autosomal dominant AD (*22*). Lastly, we investigated alterations of biological pathways in FTD, as mirrored in the CSF proteome, and their association with relevant clinical parameters and cognitive decline.

RESULTS

We analyzed a total of 238 CSF samples from 71 *C9orf72* expansion carriers, 55 *GRN* mutation carriers, and 36 *MAPT* mutation carriers, including both presymptomatic and symptomatic carriers in each group, as well as 76 asymptomatic noncarriers (Table 1). Key methodological information of this study is summarized in Fig. 1, and specific descriptions for each analysis are detailed in the Materials and Methods and Supplementary Methods sections. Having prepared and analyzed all study samples using protocols previously described and developed by our laboratory (*23*–*25*), we initially explored differential protein abundances among symptomatic groups to assess widespread CSF proteomic changes in the context of different underlying pathologies and compared those with AD. Next, we used linear models to discern mutation-associated proteins already changed at the presymptomatic disease stage. Furthermore, using weighted gene coexpression network analysis (WGCNA), we aimed to elucidate pathophysiological features associated with genetic mutations, as well as the cross-sectional correlations of protein networks with measures of cognitive function and brain volume. Last, to investigate the prognostic properties of protein networks, we assessed their association with cognitive decline.

After outlier exclusion and removal of proteins with high missingness, we identified and obtained quantitative information for 1981 CSF proteins. First, we compared our TMT dataset with existing biomarker data from the same sample cohort. TMT CSF neurofilament light chain (NEFL; henceforth used interchangeably with the protein abbreviation, NfL) measurements strongly correlated with plasma NfL measurements acquired on the single-molecule array (Simoa, Quanterix) platform [correlation coefficient (r) = 0.62,

Downloaded from https://www.science.org at Universita Degli Studi Di Trento on February 10, 2025

[1]UK Dementia Research Institute at University College London, WC1N 3BG London, UK. [2]Dementia Research Centre, UCL Queen Square Institute of Neurology, University College London, WC1N 3BG London, UK. [3]Department of Psychiatry and Neurochemistry, Institute of Neuroscience and Physiology, Sahlgrenska Academy at University of Gothenburg, 431 39 Mölndal, Sweden. [4]Centre for Cognitive and Clinical Neuroscience, Division of Psychology, Department of Life Sciences, College of Health, Medicine, and Life Sciences, Brunel University, UB8 3PH London, UK. [5]Department of Neurology, Erasmus Medical Centre, 3015 GD Rotterdam, Netherlands. [6]Alzheimer's Disease and Other Cognitive Disorders Unit, Neurology Service, Hospital Clínic, Institut d'Investigacións Biomèdiques August Pi I Sunyer, University of Barcelona, 08036 Barcelona, Spain. [7]Clinique Interdisciplinaire de Mémoire, Département des Sciences Neurologiques, CHU de Québec, and Faculté de Médecine, Université Laval, Québec, QC G1V 0A6, Canada. [8]Center for Alzheimer Research, Division of Neurogeriatrics, Department of Neurobiology, Care Sciences, and Society, Bioclinicum, Karolinska Institutet, 171 64 Solna, Sweden. [9]Unit for Hereditary Dementias, Theme Aging, Karolinska University Hospital, 171 77 Solna, Sweden. [10]Fondazione Ca' Granda, IRCCS Ospedale Policlinico, 20122 Milan, Italy. [11]University of Milan, Centro Dino Ferrari, 20122 Milan, Italy. [12]Laboratory for Cognitive Neurology, Department of Neurosciences, KU Leuven, 3000 Leuven, Belgium. [13]Neurology Service, University Hospitals Leuven, 3000 Leuven, Belgium. [14]Leuven Brain Institute, KU Leuven, 3000 Leuven, Belgium. [15]Faculty of Medicine, University of Lisbon, 1649-028 Lisbon, Portugal. [16]Fondazione IRCCS Istituto Neurologico Carlo Besta, 20133 Milano, Italy. [17]University Hospital of Coimbra (HUC), Neurology Service, Faculty of Medicine, University of Coimbra, 3004-531 Coimbra, Portugal. [18]Center for Neuroscience and Cell Biology, Faculty of Medicine, University of Coimbra, 3004-531 Coimbra, Portugal. [19]Division of Neuroscience and Experimental Psychology, Wolfson Molecular Imaging Centre, University of Manchester, M20 3LJ Manchester, UK. [20]Departments of Geriatric Medicine and Nuclear Medicine, University of Duisburg-Essen, 45141 Essen, Germany. [21]Department of Neurology, Ludwig-Maximilians Universität München, 80539 Munich, Germany. [22]German Center for Neurodegenerative Diseases (DZNE), 81377 Munich, Germany. [23]Munich Cluster of Systems Neurology (SyNergy), 81377 Munich, Germany. [24]Department of Neurofarba, University of Florence, 50139 Florence, Italy. [25]IRCCS Fondazione Don Carlo Gnocchi, 50143 Florence, Italy. [26]Department of Neurology, University of Ulm, 89081 Ulm, Germany. [27]Department of Neurology, Martin-Luther-University Hospital of Halle-Wittenberg, 06120 Halle (Saale), Germany. [28]University of Lille, 59000 Lille, France. [29]Inserm 1172, Lille, 59000 Lille, France. [30]CHU, CNR-MAJ, Labex Distalz, LiCEND Lille, 59000 Lille, France. [31]Department of Psychiatry, McGill University Health Centre, McGill University, Montreal, Québec H4A 3J1, Canada. [32]McConnell Brain Imaging Centre, Montreal Neurological Institute, McGill University, Montreal, Québec H3A 0G4, Canada. [33]Nuffield Department of Clinical Neurosciences, Medical Sciences Division, University of Oxford, OX3 9DU Oxford, UK. [34]Department of Brain Sciences, Imperial College London, W12 0NN London, UK. [35]Sorbonne Université, Paris Brain Institute – Institut du Cerveau – ICM, Inserm U1127, CNRS UMR 7225, AP-HP - Hôpital Pitié-Salpêtrière, 75013 Paris, France. [36]Centre de référence des démences rares ou précoces, IM2A, Département de Neurologie, AP-HP - Hôpital Pitié-Salpêtrière, 75013 Paris, France. [37]Département de Neurologie, AP-HP - Hôpital Pitié-Salpêtrière, 75013 Paris, France. [38]Department of Clinical Neurological Sciences, University of Western Ontario, London, Ontario N6A 5A5 , Canada. [39]Tanz Centre for Research in Neurodegenerative Diseases, University of Toronto, Toronto, Ontario M5S 1A8, Canada. [40]Sunnybrook Health Sciences Centre, Sunnybrook Research Institute, University of Toronto, Toronto, Ontario M4N 3M5, Canada. [41]Department of Clinical Neurosciences, University of Cambridge, CB2 3EB Cambridge, UK. [42]Division Translational Genomics of Neurodegenerative Diseases, Hertie-Institute for Clinical Brain Research and Center of Neurology, University of Tübingen, 72076 Tübingen, Germany. [43]Center for Neurodegenerative Diseases (DZNE), 72076 Tübingen, Germany. [44]Cognitive Disorders Unit, Department of Neurology, Donostia Universitary Hospital, 20014 San Sebastian, Spain. [45]Neuroscience Area, Biodonostia Health Research Institute, 20014 San Sebastian, Gipuzkoa, Spain. [46]Department of Clinical and Experimental Sciences, University of Brescia, 25123 Brescia, Italy. [47]Department of Continuity of Care and Frialy, ASST Spedali Civili Brescia, 25123 Brescia, Italy. [48]Clinical Neurochemistry Laboratory, Sahlgrenska University Hospital, SE-43180 Mölndal, Sweden. [49]Institut du Cerveau et de la Moelle épinière (ICM), Pitié-Salpêtrière Hospital, Sorbonne Université, 75013 Paris, France. [50]University of Science and Technology of China and First Affiliated Hospital of USTC, Hefei, Anhui, P.R. China. [51]Department of Neurodegenerative Disease, UCL Institute of Neurology, Queen Square, WC1N 3BG London, UK. [52]Hong Kong Center for Neurodegenerative Diseases, Clear Water Bay, Hong Kong, China. [53]Wisconsin Alzheimer's Disease Research Center, University of Wisconsin School of Medicine and Public Health, University of Wisconsin-Madison, Madison, WI 53792, USA.
*Corresponding author. Email: a.sogorb-esteve@ucl.ac.uk
†These authors contributed equally to the work.
‡GENFI investigators are listed at the end of the paper.

Table 1. Baseline demographic characteristics of the GENFI cohort.

Characteristic	Overall, *N* = 238*	Noncarrier, *N* = 76*	Presymptomatic *C9orf72*, *N* = 44*	Presymptomatic *GRN*, *N* = 38*	Presymptomatic *MAPT*, *N* = 25*	Symptomatic *C9orf72*, *N* = 27*	Symptomatic *GRN*, *N* = 17*	Symptomatic *MAPT*, *N* = 11*	*P* value†
Age, years	48 (38, 58)	43 (38, 53)	43 (33, 50)	50 (37, 56)	42 (33, 46)	58 (55, 70)	64 (58, 67)	63 (59, 66)	<0.001
Sex, male	108 (45%)	33 (43%)	19 (43%)	18 (47%)	9 (36%)	16 (59%)	8 (47%)	5 (45%)	0.8
Education, years	15 (12, 16)	15 (12, 17)	14 (12, 16)	15 (13, 16)	15 (13, 16)	13 (11, 14)	14 (9, 15)	13 (12, 16)	0.019
Plasma NfL, pg/ml	8 (6, 15)	7 (5, 10)	8 (6, 10)	8 (5, 10)	6 (5, 9)	40 (21, 55)	44 (37, 69)	20 (18, 23)	<0.001
MMSE	30.0 (28.0, 30.0)	30.0 (29.0, 30.0)	30.0 (29.0, 30.0)	30.0 (29.0, 30.0)	30.0 (29.0, 30.0)	26.0 (20.3, 28.8)	23.0 (20.5, 28.0)	24.5 (17.8, 27.0)	<0.001
FTLD-CDR-SOB	0.0 (0.0, 1.0)	0.0 (0.0, 0.0)	0.0 (0.0, 0.5)	0.0 (0.0, 0.0)	0.0 (0.0, 0.5)	11.5 (4.8, 15.5)	10.0 (4.8, 13.0)	7.5 (3.3, 10.6)	<0.001

*Median (IQR); *n* (%). †Kruskal-Wallis rank sum test; Fisher's exact test.

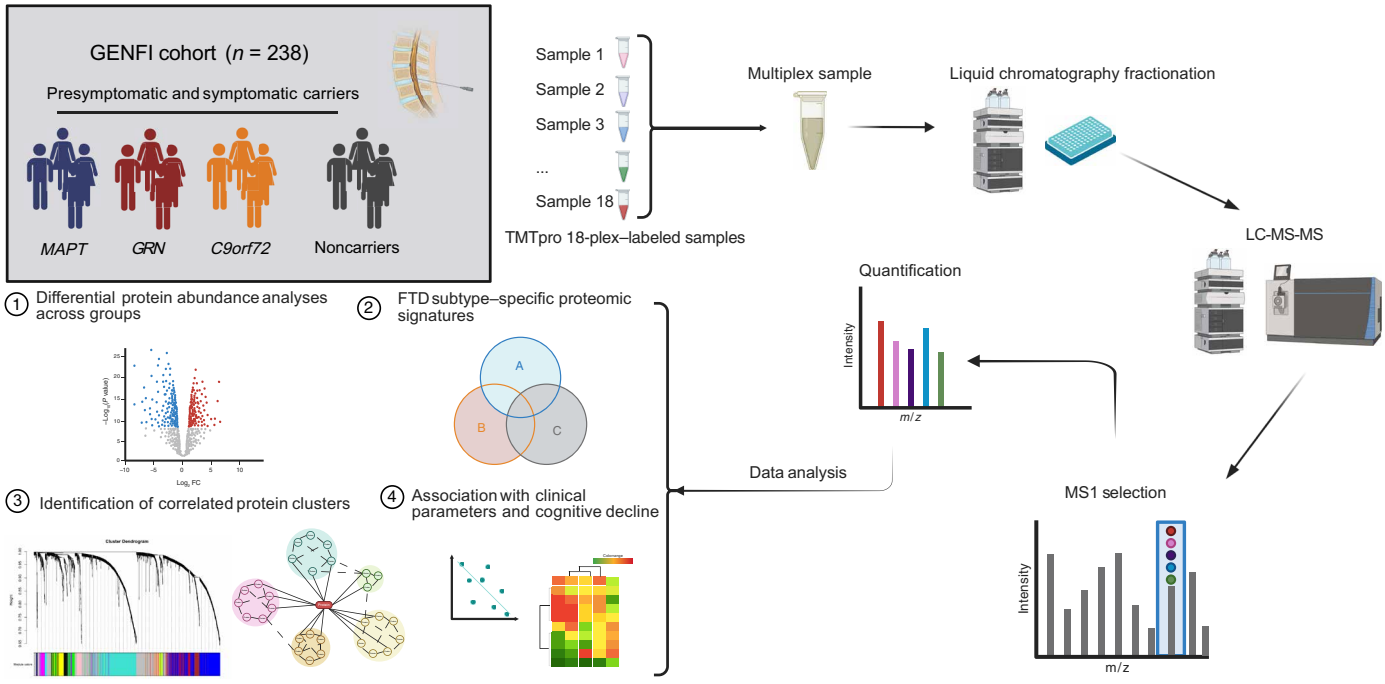

Fig. 1. Key information about participants, proteomics workflow, and data analysis. This figure shows the TMT MS/MS proteomics workflow, in which samples were preprocessed and labeled with 18 different isobaric TMTpro tags (TMTpro 18-plex) and combined into multiplex samples to allow for relative quantification and simultaneous analysis of the 18 individual samples. This process was then repeated until all 238 samples were labeled with isobaric tags. Next, each multiplex sample was fractionated using offline high-pH high-performance liquid chromatography (HPLC) to reduce sample complexity, and each fraction was subsequently analyzed by LC-MS/MS. The data analysis conceptually consisted of four steps: 1) investigating differences in protein abundances in mutation carriers compared with noncarriers and 2) determining FTD-subtype–specific proteomic signatures using linear models, 3) protein network analysis to investigate mutation- and pathology-specific pathophysiological features, and, finally, 4) correlating these protein clusters with clinical parameters and cognitive decline to discern clinically relevant changes.

$P < 0.001$; fig. S1A]. The relative protein abundances of 14-3-3 epsilon (YWHAE) ($r = 0.39$, $P < 0.001$; fig. S1B), neuronal pentraxin 2 (NPTX2) ($r = 0.8$, $P < 0.001$; fig. S1C), and neuronal pentraxin receptor (NPTXR) ($r = 0.68$, $P < 0.001$; fig. S1D) also correlated significantly with previous data from the same cohort, acquired using targeted mass spectrometric analysis (*26*). The strong correlations of TMT relative protein abundances with measures acquired on two independent platforms indicate good analytical precision of our results.

CSF proteomes differ across symptomatic FTD mutation carrier groups

Linear regression analysis, including age and sex as covariates, was used to perform group comparisons between noncarriers and

Downloaded from https://www.science.org at Universita Degli Studi Di Trento on February 10, 2025

symptomatic mutation carriers. In the case of symptomatic *MAPT* mutation carriers, 58 proteins significantly differed in abundance compared with noncarriers (Fig. 2A and table S1A), whereas the abundance of 138 and 385 proteins was significantly altered in symptomatic *GRN* (Fig. 2B and table S1B) and *C9orf72* mutation carriers (Fig. 2C and table S1C) compared with noncarriers, respectively ($P_{adjust} < 0.05$).

Next, to strengthen our findings, we compared our results with those from an external cohort consisting of symptomatic *GRN* carriers ($n = 11$) and healthy noncarriers ($n = 12$) (*27*) whose CSF proteomes were measured with label-free MS. Most proteins were commonly quantified in both studies, of which 73 proteins were significantly changed in both datasets ($P_{unadjusted} < 0.05$) (fig. S2 and table S2), with $\log_2$ fold changes being strongly correlated between the studies ($r = 0.87$, $P < 0.001$) (fig. S2).

From the 25 hits that presented the lowest *P* values in each symptomatic mutation group (table S3), a list of proteins was compiled (excluding overlap between groups) denoting corresponding protein abundance fold changes compared with noncarriers in a heatmap (Fig. 2D and table S3). As expected, the three neurofilaments, NfL, NfM, and NfH, alongside YKL-40 (CHI3L1), exhibited the greatest fold change in abundance across most symptomatic groups when compared with noncarriers, with NfL abundances being up to 7.4 times higher in symptomatic *GRN* carriers in comparison with noncarriers. Other proteins showing a notable positive fold change in symptomatic mutation carriers included the spectrins (SPTBN1 and SPTAN1) as well as UCHL1, FABP3 (fatty acid–binding protein 3), PEA15 (proliferation and apoptosis adaptor protein 15), and several 14-3-3 proteins (YWHAZ, YWHAG, YWHAE). Proteins that were lower in abundance across symptomatic mutation carriers compared with noncarriers included the synaptic proteins NPTXR, NPTX2, and NPTX1, as well as proprotein convertase subtilisin/kexin type 2 (PCSK2) and proenkephalin (PENK). Furthermore, GRN relative abundance levels were lower in *GRN* mutation carriers. Most proteins showed the same directionality of abundance fold change across the three mutation carrier groups except for a few proteins. These included GRN, which showed an opposite direction of change in symptomatic *C9orf72* and *GRN* carriers (both $P_{adjust} < 0.05$), and the lysosomal proteins deoxyribonuclease 2 (DNASE2) and phospholipase B domain containing 2 (PLBD2), which were selectively decreased in symptomatic *MAPT* carriers.

Proteomic similarities and differences between genetic FTD and sporadic AD

Because some of the proteins quantified in this study are expected to change also in other neurodegenerative disorders, we compared the summary statistics of our differential abundance analyses of symptomatic FTD mutation carrier groups with summary statistics of previously published TMT proteomics datasets from two distinct AD studies: the European Medical Information Framework (EMIF) CSF study (*25*) and a CSF proteomics study performed by Higginbotham and colleagues (*28*). Of the about 1192 proteins quantifiable in all three studies (Fig. 3A and tables S4, A and B, and S5), only 6 were significantly changed in all groups ($P_{adjust} < 0.05$) (YWHAZ, YWHAG, UCHL1, NPTXR, NPTX2, and FABP3; Fig. 3, B and C, and table S5). Conversely, many proteins were distinctly changed in each FTD mutation carrier group (Fig. 3, B and C, and table S5), with more widespread changes being found in symptomatic *C9orf72* carriers [calretinin (CALB2), sortilin 1 (SORT1), and roundabout guidance receptor 1 (ROBO1)] compared with *GRN* [transmembrane protein 132A (TMEM132A), ring finger protein (RNF13), and chitinase 3–like 2 (CHI3L2)] and *MAPT* carriers [hexosaminidase subunit alpha (HEXA), semaphorin 6A (SEMA6A), and cathepsin D (CTSD)]. Proteins shared between *C9orf72* and *GRN* carriers included many proteins involved in lysosomal processes [GRN, cathepsin S (CTSS), and lysosomal-associated membrane protein 1 (LAMP1)]. Proteins uniquely changed in both AD studies included neurogranin (NRGN) and SPARC-related modular calcium binding 1 (SMOC1), both previously shown to increase in response to amyloid pathology (*29*). Only two proteins were distinctly changed in all symptomatic FTD mutation carrier groups [CD44 and follistatin like 4 (FSTL4)], likely reflecting the different processes involved in these disease-causing mutations.

Mutation-associated proteomic changes are evident in presymptomatic disease mutation carriers

Having compared proteomic alterations of symptomatic FTD subtypes and their overlap with AD, we next set out to determine changes in protein abundances associated with a specific genetic background, regardless of affectation (presence or absence of symptoms). The presence of symptoms is expected to coincide with diverse neurodegenerative processes affecting the CSF proteome and obscuring potential mutation-related changes. Thus, to investigate proteomic alterations attributable to each underlying pathogenic mutation, we (i) fitted linear models combining all study participants, testing the effect of genetic mutation on protein abundances while adjusting for affectation (Fig. 4 and table S6) and (ii) compared CSF proteomes of presymptomatic individuals with noncarriers for each genetic group separately (figs. S3 to S8 and table S7, A to C). This approach yielded several proteins strongly associated with the *C9orf72* (Fig. 4A), *GRN* (Fig. 4B), or *MAPT* (Fig. 4C) mutation status, of which the top five proteins for each association were chosen for visual display. Standardized β coefficients indicate the strength of the association and are depicted in a forest plot for ease of comparison. The protein most strongly associated with the *C9orf72* mutation status was CALB2 (Fig. 4A; standardized $\beta = 0.77$, $P_{adjust} < 0.01$), which could also be found among the top changed proteins in the analysis of presymptomatic *C9orf72* carriers versus noncarriers (figs. S5 and S8). Numerous proteins found to be associated with *C9orf72*, such as glucose-6-phosphate isomerase, hexokinase 1 (HK1) (Fig. 4A and fig. S8), and phosphoglycerate kinase 1 (PGK1) (fig. S8) are key enzymes of the glycolysis pathway, hinting at early metabolic disturbances. The proteins CALB2, HK1, and PGK1 demonstrated a stepwise increase in abundance from noncarriers over presymptomatic to symptomatic *C9orf72* carriers (fig. S8), further underlining their implication in *C9orf72*-related disease processes.

Reflecting the GRN haploinsufficiency, the protein most strongly associated with *GRN* mutation status was GRN itself (Fig. 4B and figs. S4 and S7; standardized $\beta = -1.59$, $P_{adjust} < 0.01$), followed by alpha-*N*-acetylgalactosaminidase (NAGA) (standardized $\beta = 0.71$, $P_{adjust} = 0.04$) and RNF13 (standardized $\beta = 0.64$, $P_{adjust} = 0.09$). RNF13, although narrowly failing to reach the significance threshold of 0.05 after multiple testing corrections in the combined analysis, was found to be significantly changed in the presymptomatic *GRN* carrier versus noncarrier analysis (fig. S4; $P_{adjust} = 0.03$) and increased in abundance across the *GRN* disease continuum (fig. S7). The proteins most strongly associated with *MAPT* mutation status were PEA15 (Fig. 4C; standardized $\beta = 0.9$, $P_{adjust} < 0.01$) and

Downloaded from https://www.science.org at Universita Degli Studi Di Trento on February 10, 2025

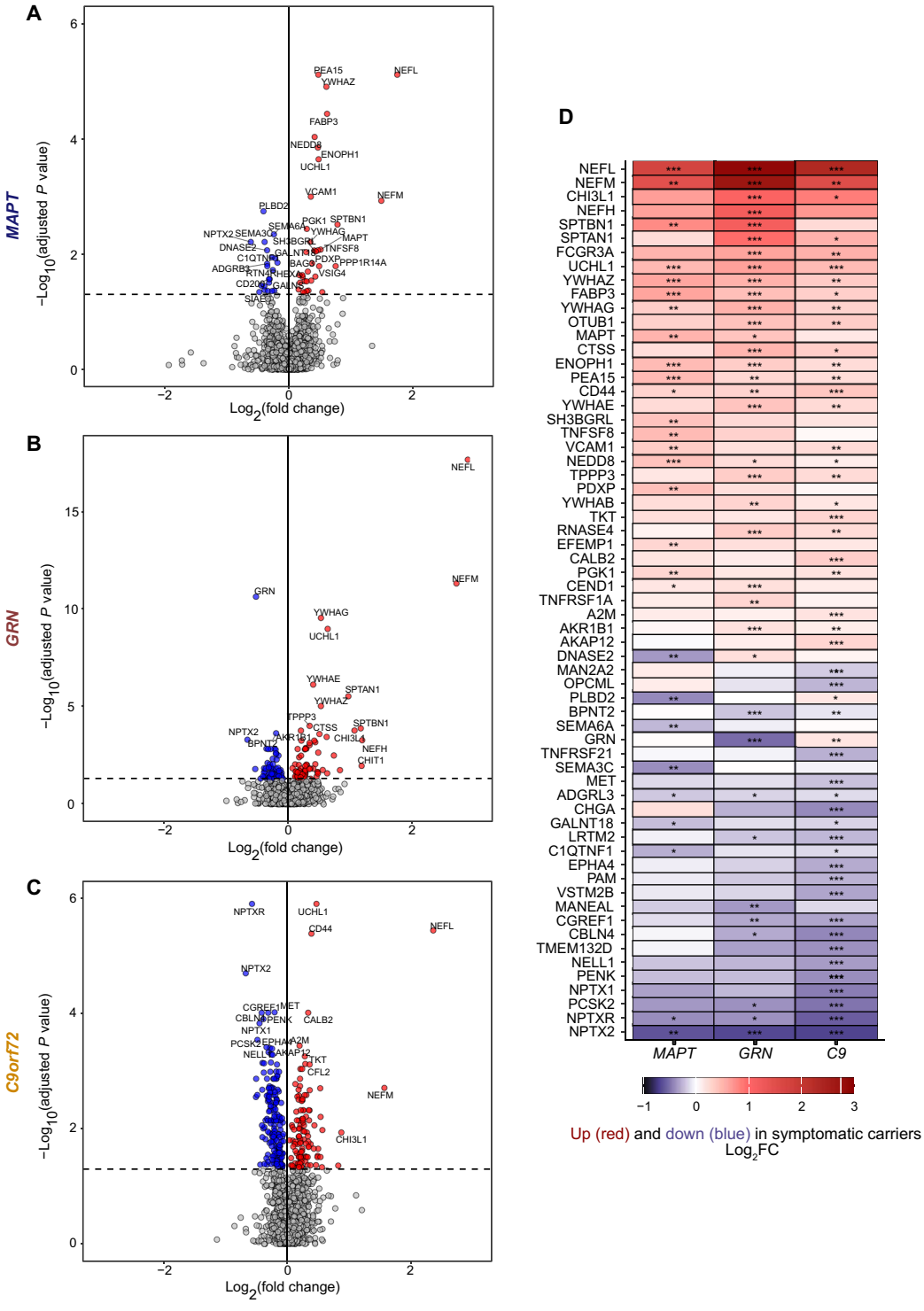

Fig. 2. Volcano plots and heatmap displaying top protein hits in symptomatic mutation carriers versus noncarriers. (**A** to **C**) Volcano plots showing proteomic differences in symptomatic *MAPT* (A), *GRN* (B), and *C9orf72* (C) mutation carriers on the basis of linear regression analysis with age and sex as covariates. Differences were considered significant if Benjamini-Hochberg [false discovery rate (FDR)]–adjusted *P* values were < 0.05. (**D**) The heatmap displays the 25 proteins in each group that had the lowest FDR-adjusted *P* values in linear regression analysis, resulting in 62 proteins when accounting for overlapping proteins among groups. The $\log_2$ fold abundance change between noncarriers and the respective mutation carrier group is color coded; proteins higher or lower in abundance in symptomatic mutation carriers versus noncarriers are shown in red and blue, respectively. Note that not all proteins listed in (D) were significantly altered in all groups. *P_{adjust} < 0.05, **P_{adjust} < 0.01, and ***P_{adjust} < 0.001. Details on exact *P* values and $\log_2$ fold change can be found in tables S1A to S1C.

Downloaded from https://www.science.org at Universita Degli Studi Di Trento on February 10, 2025

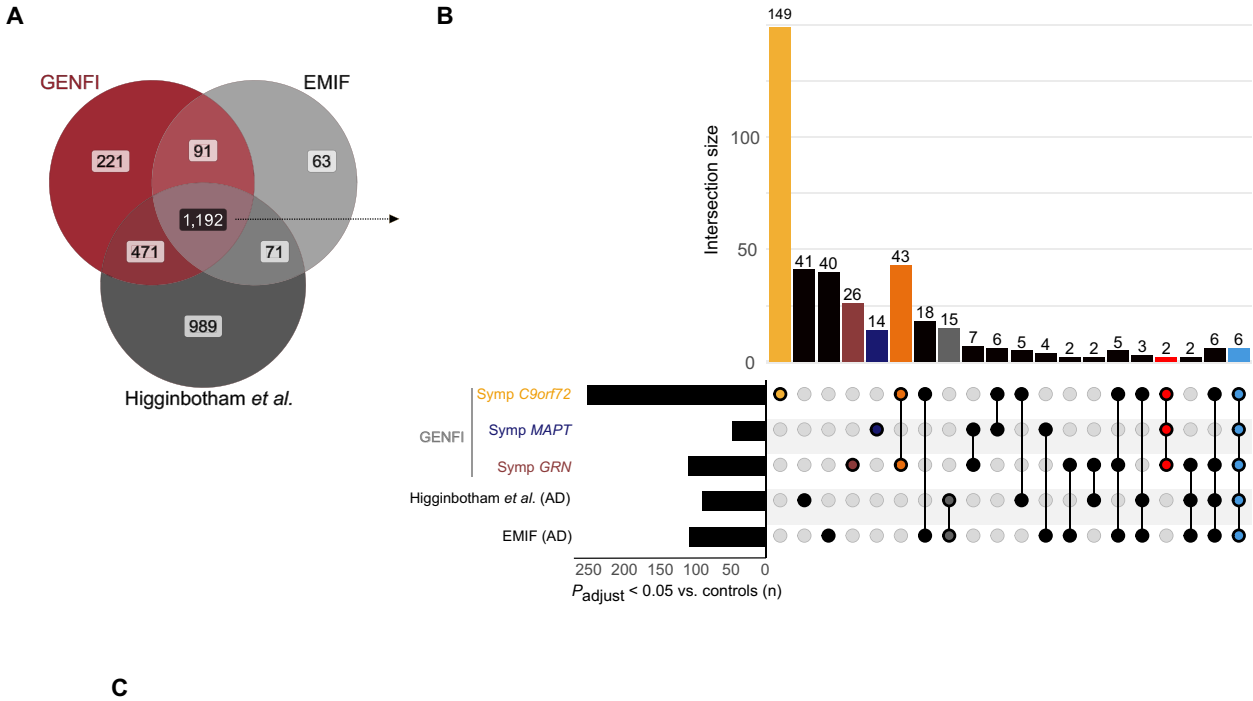

C

Symptomatic *C9orf72*	Symptomatic *MAPT*	Symptomatic *GRN*	All GENFI and both AD
SORT1, CALB2, ROBO1 (...)	HEXA, SEMA6A, CTSD (...)	TMEM132A, RNF13,CHI3L2 (...)	YWHAZ, YWHAG, UCHL1, NPTXR, NPTX2, FABP3
TDP-43 (*GRN*/*C9orf72*)	AD	All GENFI	
GRN, CTSS, LAMP1 (...)	NRGN, SMOC1, STMN1 (...)	FSTL4, CD44	

Fig. 3. Cross-cohort comparisons of symptomatic genetic FTD with AD. (**A**) Venn diagram with proteins measured in GENFI, the EMIF cohort (*25*), and Higginbotham *et al.* (*28*). The overlap ($n = 1192$) represents proteins quantified in all studies. (**B**) UpSet plot of differentially expressed proteins (FDR-adjusted $P < 0.05$) for symptomatic *C9orf72*, *MAPT*, and *GRN* mutation carriers and for patients with AD from the Higginbotham and EMIF cohorts. The upper, vertical bars show the number of differentially expressed proteins exclusive to one patient group or shared between groups. The left horizontal bars represent the total number of proteins with $P_{adjust} < 0.05$ comparing each group with control individuals. Intersections of clinical interest are color coded. Intersections only containing one protein are not displayed in the figure. (**C**) Selection of proteins in intersections from the UpSet plot in (B) that are of clinical interest, as well as proteins specifically altered in one group. Proteins included in each of these intersections, as well as those not displayed, can be found in table S5.

SEMA6A (standardized $\beta = -0.82$, $P_{adjust} < 0.05$). PEA15 was also significantly altered in the comparison between presymptomatic *MAPT* carriers and noncarriers (fig. S3, $P_{adjust} = 0.02$) and increased in abundance from the presymptomatic to symptomatic disease stage (fig. S6). Because of concerns of family membership adversely affecting our results, we conducted sensitivity analyses adopting the same linear models as in the main analysis but including one member from each family. These analyses presented similar results (table S8, A to E).

Protein networks reveal pathology-specific pathophysiological alterations and correlate with clinical parameters

Having studied the proteomic signatures of each genetic group, we further explored the biological processes implicated in these proteomic changes by performing WGCNA (figs. S9 to S23). WGCNA is an analysis tool aimed at reducing the complexity of a proteomics dataset by breaking it down into gene ontology (GO)–annotated protein clusters. These protein modules consist of highly co-correlated proteins likely reflecting similar biological processes. We identified a total of 14 protein modules, including a group of 645 proteins that could not be assigned to any of the modules and a module containing contaminants from the laboratory environment. The modules varied in size from 14 to 349 proteins with a median module size of 52 proteins (table S9). We determined the biological relevance of each protein module using GO analysis of its constituent proteins and selected the most representative term for module annotation (figs. S12 to S23). Furthermore, we identified the hub proteins of each module, indicating the proteins most strongly correlating ($R > 0.7$) with the module's first principal component (eigenprotein value), as most representative and important proteins of the respective module.

Figure 5A shows a selection of six protein modules and their corresponding eigenprotein values (representative abundance values) plotted across all genetic groups as well as noncarriers. One module, which we termed "core markers" of neurodegenerative disease, consisted of 15 proteins and was most strongly increased in abundance in each genetic group at the symptomatic stages when compared with noncarriers. The strong difference between noncarriers and presymptomatic *MAPT* carriers was largely influenced by age. It included YWHAG, NEFL, CHI3L1, NEFM, and YWHAZ as hub

Downloaded from https://www.science.org at Universita Degli Studi Di Trento on February 10, 2025

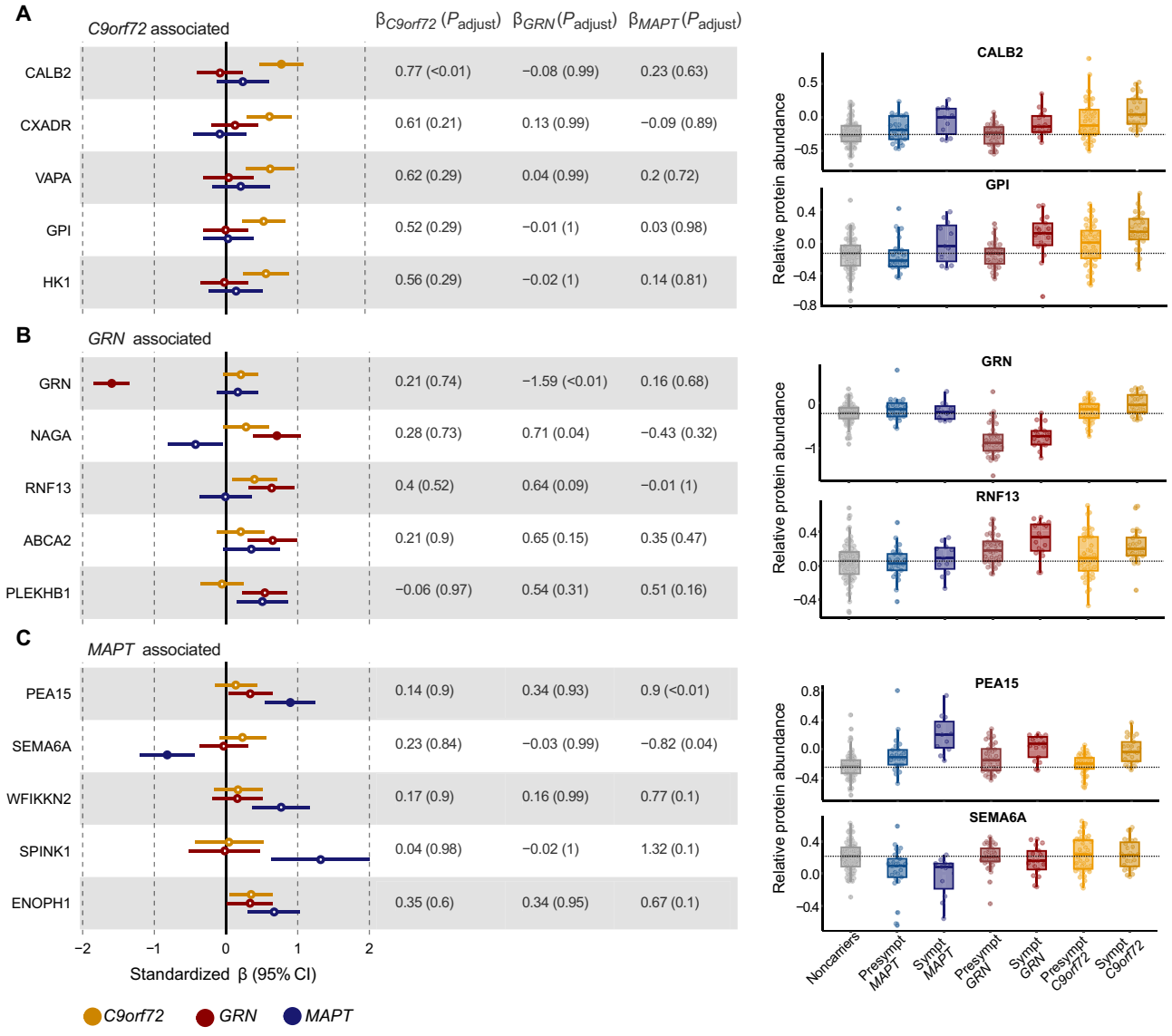

Fig. 4. Identification of mutation-associated proteins. (**A** to **C**) Left, forest plots of the top five proteins most strongly associated with *C9orf72* (A), *GRN* (B), and *MAPT* (C) mutation. For the identification of mutation-associated proteins, linear models were fitted testing the effect of mutation carrier group on protein abundance, including affectation (presence/absence of symptoms) as well as age and sex as covariates. Noncarriers served as a reference group. Coefficients with an adjusted $P < 0.05$ are depicted as colored points, and 95% confidence intervals (CIs) were added. Standardized β estimates including corresponding Benjamini-Hochberg–adjusted *P* values for each association and mutation group are reported. Right, box plots of two manually selected proteins across the entire cohort. The dotted line denotes the median $\log_2$-transformed protein abundance value of the noncarrier group.

proteins. These proteins were also among the top hits in the differential abundance analysis and had the highest fold change in symptomatic mutation carriers compared with noncarriers (Fig. 2D). As expected, many proteins belonging to the core markers module were also seen among the proteins overlapping between the three genetic forms and were found to be altered in the CSF of patients with AD in the EMIF and Higginbotham studies (Fig. 3, B and C).

Correlating the core marker eigenprotein values with clinical parameters in both presymptomatic and symptomatic mutation carriers (Fig. 5B) revealed a strong positive association of the module with both plasma NfL ($r = 0.86$, $P_{adjust} < 0.0001$) and the National Alzheimer's Coordinating Center (NACC) FTLD plus clinical dementia rating (CDR) sum of boxes (SOB) (FTLD-CDR-SOB) disease severity scores ($r = 0.67$, $P_{adjust} < 0.0001$) as well as a negative association with mini mental state examination (MMSE) scores ($r = -0.53$, $P_{adjust} < 0.0001$) and regional brain volumes. The core markers module also positively correlated with estimated years until disease onset (EYO) in presymptomatic individuals ($r = 0.68$, $P_{adjust} < 0.0001$).

Besides the core markers module, eigenprotein values for both the "actin binding" module and the "stress response" module were higher across symptomatic mutation carrier groups (albeit not statistically significant), suggesting common pathophysiological alterations in these processes (Fig. 5A). Both modules, along with the

Downloaded from https://www.science.org at Universita Degli Studi Di Trento on February 10, 2025

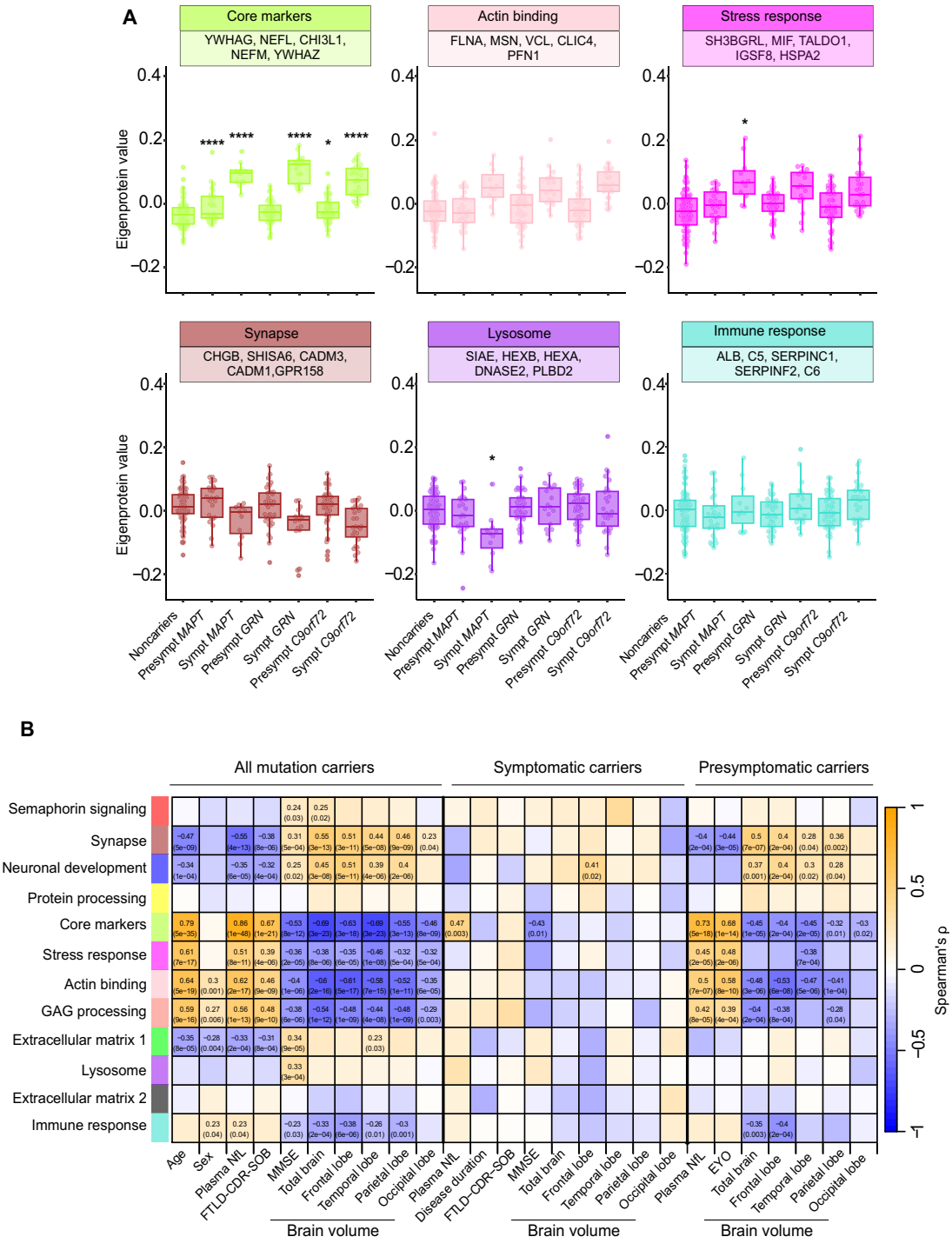

Fig. 5. Weighted gene coexpression network modules show mutation/pathology-specific changes and correlate with relevant clinical parameters. (**A**) WGCNA identified 14 distinct highly correlated modules of proteins. Modules were named in accordance with GO terms mapped to their constituent proteins. Six modules of particular interest were selected, and their eigenprotein values were plotted across the entire cohort: core markers, actin binding, stress response, synapse, lysosome, and immune response. Framed boxes contain the names of the top five hub proteins of each module, as determined by having the highest module membership value (kME). *P* values for respective group comparisons versus noncarriers are derived from linear regression analyses with Tukey's post hoc test to adjust for multiplicity. Box plots of the remaining modules can be found in fig. S24. **P* < 0.05, ***P* < 0.01, ****P* < 0.001, and *****P* < 0.0001. (**B**) Heatmap of correlation parameters of module eigenproteins with different clinical measures. Spearman's rho values are color coded, and the corresponding Bonferroni-corrected *P* values are included in parentheses for each tile. To evaluate the association of protein modules with clinical parameters at different time points of the disease continuum, correlations were performed in an indicated subset of individuals only. GAG, glycosaminoglycan.

Downloaded from https://www.science.org at Universita Degli Studi Di Trento on February 10, 2025

"glycosaminoglycan processing" module (fig. S24D), showed a similar correlation pattern to the core markers module.

Conversely, the "synapse" module, containing proteins such as CHGB, SHISA6, CADM3, CADM1, and GPR158, showed lower eigenprotein values in all symptomatic mutation carrier groups compared with noncarriers, although changes were not significant. Its correlation pattern with clinical parameters was inverse compared with the core markers module, exhibiting negative correlations with age, plasma NfL, and FTLD-CDR-SOB scores, and positive correlations with MMSE scores and brain volumes (Fig. 5B), similarly to the "neuronal development" and the "extracellular matrix 1" modules (fig. S24, B and E). The neuronal development module contained several proteins considered to be markers of synaptic loss (NPTX2 and NPTXR, among others) and was significantly lower in symptomatic *C9orf72* carriers ($P_{adjust} < 0.05$).

We also identified a module associated with lysosomal proteins ("lysosome" module), for which eigenprotein values were selectively decreased in symptomatic *MAPT* mutation carriers compared with noncarriers ($P_{adjust} < 0.05$). They were also slightly decreased in presymptomatic *MAPT* individuals, albeit without statistical significance ($P = 0.79$). The hub proteins were determined to be sialic acid acetylesterase (SIAE), HEXB, HEXA, DNASE2, and PLBD2, all of which are implicated in lysosomal processes. These specific changes in *MAPT* mutation carriers in DNASE2 and PLBD2 were already evident in the heatmap (Fig. 2D) contrasting symptomatic mutation carrier groups. Other lysosomal proteins found to be commonly changed in *GRN* and *C9orf72* carriers (LAMP1 and CTSS; Fig. 3) were not part of the lysosome module, suggesting different subpopulations of lysosomal proteins, which might be reflective of distinct biological processes. The lysosome module did not correlate with markers of neurodegeneration, cognitive decline, or brain atrophy.

The "immune response" module contained proteins related to the complement pathway and the immune system. For all symptomatic groups, there was a visible trend of increase in these clusters when compared with noncarriers; however, these differences were not statistically significant ($P > 0.05$). This module showed similar correlation patterns with clinical features to the core markers module.

Protein networks associate with cognitive decline in mutation carriers

To evaluate the prognostic properties of protein networks, the module eigenprotein values of mutation carriers with cognitive evaluation at the time of lumbar puncture (LP) ($n = 146$, mean number of annual visits = 2.7, range 1 to 5) were modeled with the FTLD-CDR-SOB score as outcome. In agreement with analyses of cross-sectional cognitive scores, higher core markers eigenprotein values were most strongly associated with higher FTLD-CDR-SOB scores, reflecting poorer cognitive outcomes (standardized $\beta = 0.83$, $P < 0.001$; Fig. 6A). A similar but less prominent pattern was seen for the actin binding module (standardized $\beta = 0.50$, $P < 0.001$; Fig. 6B). Conversely, lower eigenvalues of the synapse module were associated with increasing FTLD-CDR-SOB scores (standardized $\beta = -0.49$, $P < 0.001$; Fig. 6C). This indicated that lower synapse eigenprotein values were associated with worse cognitive outcomes. Further, the "semaphorin signaling," neuronal development, extracellular matrix 1, lysosome, and immune response module eigenprotein values were also significantly (all $P < 0.05$) associated with cognitive decline (Fig. 6D; for full model output, see table S10).

DISCUSSION

The present study offers a detailed and untargeted account of the CSF proteomic signatures in genetic FTD. By including participants from the well-characterized GENFI cohort, with presymptomatic and symptomatic carriers of pathogenic mutations in the three genes comprising the overwhelming majority of genetic FTD, we covered most of the clinical continuum as well as its underlying genetic causes. Our analytical approach allowed us to uncover proteomic changes beyond known CSF and blood biomarkers, such as NfL, glial fibrillary acidic protein, and progranulin, suggesting potential pathology- and FTD-specific biomarkers.

To assess both differences and similarities across the FTD spectrum, we explored the proteome of each genetic group through separate analyses. Using differential protein abundance analysis, we found several proteins that were altered in all symptomatic mutation carriers. Among these proteins, many of the top hits were neuronal proteins known to be increased in CSF in several neurodegenerative diseases, including neurofilaments (NfL, NfM, and NfH) and 14-3-3 proteins (YWHAZ and YWHAG) (*17*, *18*, *30*). NfL (both when measured in CSF and plasma) has especially been suggested to be of diagnostic, prognostic, and theragnostic value in FTD because both this and other studies have found large fold changes (seemingly most pronounced in *GRN* carriers) compared with healthy controls and even other brain-related conditions, which bears important implications for differential diagnoses (*7*, *30*, *31*). The decreased relative abundances of neuronal pentraxins (NPTX1 and NPTX2) and their receptor (NPTXR), previously reported to be decreased in genetic FTD (*15*, *26*, *32*) and other neurodegenerative diseases (*18*, *33*), further emphasize the presence of synaptic changes in FTD. These markers displayed a similar fold change in the study of FTD-*GRN* by Pesämaa *et al.* (*27*), which we used to validate our findings. In addition, changes shared between groups included proteins recently suggested to be associated with astrocytic and microglial responses in AD as well as FTD-TDP brains, such as rab GDP dissociation inhibitor alpha (GDI1), FABP3, and CD44 (*34*). Although not significantly changed in either the EMIF or Higginbotham study, CD44 antigen has been shown to play a role in neuroinflammation in AD, in relation to disease-associated microglia (*34*, *35*) and their communication with astrocytes (*36*), as well as in *GRN*-deficient animal models (*37*). Despite not being specific to glial responses in FTD, the increases seen in symptomatic FTD suggest that CD44 may be a promising fluid-based marker to index such glial changes in future trials. GDI1, FABP3, and CD44 were also identified as microglia activation–dependent markers in the study by Pesämaa *et al.* (*27*).

Many of the proteins found to be altered in all groups of symptomatic carriers were assigned to the core markers module in the protein network analysis (YWHAG, NfL, UCHL-1, FABP3, CHI3L1, and CD44). Several of these core marker proteins (FABP3, UCHL1, and YWHAG, among others) were also shown to be changed in abundance in the CSF of patients with AD, as evidenced by the EMIF and Higginbotham studies (*25*, *28*). Together, these findings support the strong neurodegenerative and glial component of both diseases and highlight that, despite AD and FTD being separate disease entities, they appear to share common downstream pathophysiological features. The core markers also reflected disease severity and imaging measures of neurodegeneration and proved to be the protein network most closely linked to cognitive decline and EYO, highlighting the prognostic value of markers reflecting neurodegenerative and neuroinflammatory processes.

Downloaded from https://www.science.org at Universita Degli Studi Di Trento on February 10, 2025

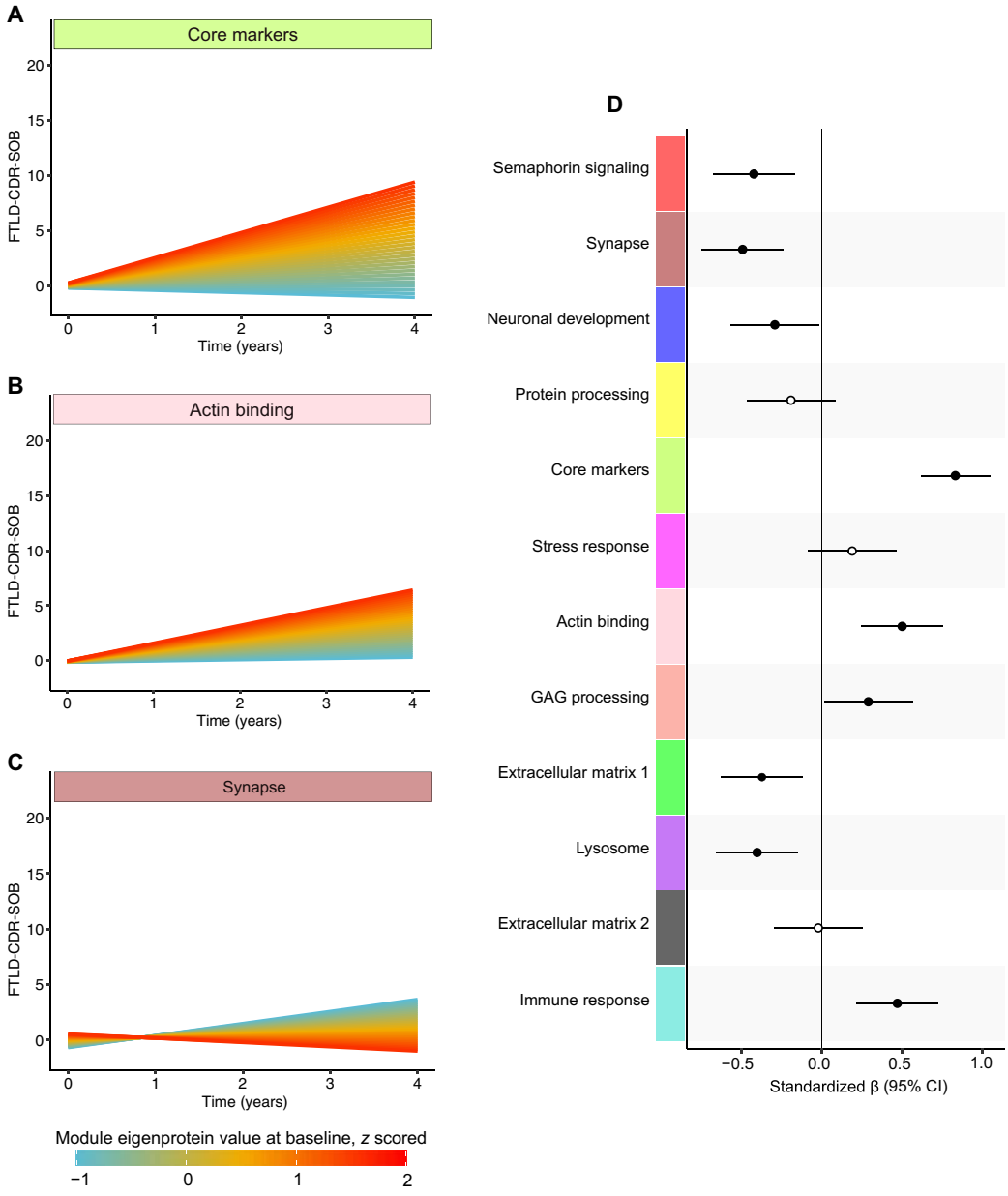

Fig. 6. Weighted gene coexpression network modules predict cognitive change in genetic FTD. The plots show estimates of the fixed effect (standardized module eigenprotein value times time in years from baseline) of linear mixed effects models with the FTLD-CDR-SOB score as the dependent variable in mutation carriers (n = 146). The models included standardized eigenprotein values times time, age, sex, years of education, and affectation at baseline (presymptomatic/symptomatic) as independent variables. (**A** to **C**) Estimates of ME values for core markers (A), actin binding B), and synapse (C) modules from separate models. The colors visualize the estimated cognitive trajectories at z-scored baseline eigenprotein values ranging from −1 to 2 SD from the mean. (**D**) Forest plot of the standardized β estimates and 95% CIs of each module eigenprotein value times time. The filled points denote statistically significant ($P < 0.05$) interaction terms.

Besides the core markers module, we identified several other protein modules seemingly altered across groups in the FTD spectrum compared with noncarriers, with constituent proteins relating to the synapse (synapse module), in line with results shown in the heatmap (Fig. 2), actin binding, and stress response. Lower relative abundances of the synapse eigenprotein values also predicted cognitive decline in mutation carriers. Although these protein networks strongly correlated with clinical and neuroimaging features, abundance differences compared with noncarriers were rendered nonsignificant, likely because of their association with age. The synaptic protein neurogranin (NRGN) as well as the extracellular matrix protein SMOC1 were not altered in any of the groups of symptomatic genetic FTD mutation carriers but altered in both AD studies. This is in line with previous research (*29*) and suggests their specificity for amyloid-related changes in AD. Conversely, the protein FSTL4 was found to be changed in all groups of symptomatic FTD mutation carriers but not AD, hinting at its potential specificity for FTD. Knowledge is still limited on the extent to which this protein is associated with

Downloaded from https://www.science.org at Universita Degli Studi Di Trento on February 10, 2025

neurodegenerative disorders, although one small study reported lower protein abundances of FSTL4 in patients with ALS (*38*).

Because this study aimed to look beyond proteomic alterations shared between FTD subtypes as well as AD, we also investigated the differences across genetic forms of FTD and their expected underlying pathologies. We identified lysosomal proteins with the potential to separate processes implicated in *MAPT* mutation carriers but not the other two groups. Decreased DNSAE2 and PLBD2 (which show divergent patterns in symptomatic *GRN* and *C9orf72* carriers as shown in Fig. 2B) appeared to be specifically related to the presence of tau pathology, without the amyloid background observed in AD (as evident in Fig. 3). This was further supported by PLBD2 and DNASE2 being among the hub proteins in the lysosome module, driving the marked eigenprotein value decrease in *MAPT* mutation carriers (Fig. 5G). Evidence suggests that PLBD2 and DNASE2 play a role in lysosomal processes (*39*–*42*). These results were unexpected, given the evidence of lysosomal dysfunction in *GRN* mutation carriers, but not in *MAPT* mutation carriers, because of the role of progranulin in the endolysosomal pathway (*43*, *44*). Nonetheless, tau protein has been previously implicated in the trafficking of autophagic vesicles and autolysosome fusion (*45*–*47*), suggesting that a reduction in proteins related to the endolysosomal pathway in *MAPT* may indicate a potential dysregulation in this system. Lysosomal acid phosphatase 2 (ACP2) (*48*), a member of the lysosome module, was found to be decreased in presymptomatic *MAPT* carriers, which aligns with the changes seen in the protein networks in symptomatic carriers. This dysregulation might be different from that observed in *C9orf72* and *GRN* carriers, in which there was a selective increase in some lysosomal proteins (LAMP1 and CTSS) not belonging to the lysosome module and thus displaying a different correlation pattern.

In analyses stratifying groups by mutation irrespective of symptomatology, we observed a stepwise abundance increase across the disease continuum in PEA15, an astroglial protein associated with glial responses (*34*), being more strongly associated with *MAPT* mutation carriership than with *GRN* and *C9orf72*. In *GRN* carriers, the expected decrease in GRN concentrations was observed (*10*) in both presymptomatic and symptomatic *GRN* carriers. Further, we found increased concentrations of RNF13 in both presymptomatic and symptomatic *GRN* carriers, which might reflect an underlying alteration in the ubiquitin system (*49*), not as well captured in *MAPT* and *C9orf72* carriers. We found several proteins that were changed in *C9orf72* expansion carriers, including PGK1, which not only was elevated in presymptomatic carriers in comparison with noncarriers but also showed a stepwise increase across the disease continuum. In addition, CALB2 as well as HK1 were elevated in presymptomatic *C9orf72* carriers, and, like PGK1, their relative abundances appeared to increase with disease progression. Both HK1 and PGK1 are key enzymes of the glycolysis pathway, suggesting that a dysregulation of glucose metabolism might be an early feature of *C9orf72*-related FTD (*50*). HK1 and CALB2 were also selected as two of the top proteins in analyses comparing mutation carriers irrespective of underlying symptomatology, indicating their stronger association with a *C9orf72* mutation.

This study has limitations. The identification of a lower number of proteins that were changed in *MAPT* mutation carriers in comparison with *GRN* and *C9orf72* mutation carriers may be due to a lower number of participants in this group. *C9orf72* seems to be the most common genetic cause of FTD worldwide, followed by *GRN* and then *MAPT* (*1*), and this trend is reflected in the recruitment of the GENFI study. Because of the structure of participant recruitment in the GENFI cohort, some participants from the same family were included in the study. Family members may share genetic and environmental factors to a greater degree than the general population, which may bias the results. However, we conducted sensitivity analyses that included only one member from each family, with comparable results.

Although genetic FTD offers the unique advantage of linking proteomic changes to pathological alterations antemortem, specifically distinguishing between tau and TDP-43 pathology, it cannot be excluded that observed proteomic changes are specific to the underlying genetic mutation and not necessarily transferable to the resulting pathology in sporadic FTD. Further, although both the EMIF and Higginbotham *et al.* studies used similar statistical and mass spectrometric methods, it is likely that some of the differences seen between studies are due to varying power to detect proteomic alterations.

Last, the age difference between symptomatic carriers and noncarriers may have resulted in age influencing the interpretation of results. However, including age as a covariate in all relevant analyses is likely to mostly mitigate this potential issue.

To conclude, this study explored the CSF proteome in genetic FTD and found distinct changes occurring already in presymptomatic mutation carriers indicating early lysosomal dysfunction and alterations in proteins involved in glucose metabolism, with more widespread proteomic differences during the symptomatic stage of the disease. We found that proteomic profiles largely overlapped between the different causes of FTD as well as with AD, especially with respect to synaptic loss, glial responses, and neurodegenerative processes. Furthermore, we found that certain lysosomal proteins are strongly associated with *MAPT* mutation carriers, hinting at their potential value in distinguishing underlying FTD pathologies. Together, our results can inform the development of targeted assays that could be of value in clinical scenarios as well as in research aiming to better understand these diseases.

MATERIALS AND METHODS

Study design

The objective of this study was to explore the CSF proteomic signatures of the three most common genetic pathogenic mutations in FTD. To this end, 238 CSF samples from an ongoing case-control study cohort of genetic FTD, the GENFI cohort, were used. Participants of the GENFI cohort were recruited from 14 GENFI centers, distributed across Europe and Canada, since 2012. One CSF sample per participant, generally obtained upon the first (baseline) visit, was included in the present cross-sectional study. The samples were randomized for measurement, and the researchers were blinded for genetic status and genetic mutations at the time of the experiment. No prior calculations were performed to determine cohort size; all available samples were included in the study. The presence of batch effects and sample outliers were investigated using hierarchical clustering and principal components analysis before and after normalization. The proteomic experiments were conducted in one replicate. No participants were excluded. The London Queen Square Ethics committee as well as local ethics committees at each site approved the study. The study complied with the Declaration of Helsinki. All participants provided written informed consent at enrollment

Downloaded from https://www.science.org at Universita Degli Studi Di Trento on February 10, 2025

including consent to publication. This study adhered to the Strengthening the Reporting of Observational Studies in Epidemiology reporting guidelines for observational studies.

Participants and sample collection

Participants were recruited from the GENFI study, which includes individuals with a diagnosis of FTD due to a pathogenic mutation in *MAPT*, *GRN*, or *C9orf72* (symptomatic mutation carriers), at-risk first-degree relatives (presymptomatic mutation carriers), and noncarriers (mutation-negative first-degree relatives from the same families). Demographics of the cohort are described in Table 1.

Participants were assessed using a standardized history and examination and were classified as symptomatic if they met consensus diagnostic criteria (*51*, *52*). The CDR Dementia Staging Instrument with the NACC FTLD component was used to assess disease severity, and the CDR plus NACC FTLD SOB was used for quantitative analyses here. Participants underwent volumetric T1-weighted magnetic resonance imaging scans. More details on clinical evaluation and imaging can be found in Supplementary Methods.

CSF collection and sample preparation

CSF was collected in polypropylene tubes through LP and was centrifuged to remove insoluble material and cells. Supernatants were aliquoted and stored at −80°C within 2 hours after collection. CSF samples (25 μl) were reduced by the addition of tris(2)-carboxyethylphosphine (TCEP) in sodium deoxycholate (DOC) and triethylammonium bicarbonate (TEAB) to a final concentration of 5 mM TCEP (1% DOC and 100 mM TEAB). After incubation at 55°C for 1 hour, the samples were equilibrated to room temperature (RT). Carbamidomethylation was performed by adding iodoacetamide to a concentration of 10 mM and subsequently incubating the reaction mixture in the dark for 30 min at RT. Trypsin (100 μg per vial; Promega) was dissolved in resuspension buffer (Promega), and 1.5 μg was added for overnight digestion at 37°C. The next day, TMTpro reagents (TMT 18plex, Thermo Fisher Scientific, 5 mg) were dissolved in 200 μl of acetonitrile (ACN) having been equilibrated to RT. The samples were randomized across TMT sets, and TMT labeling was performed by adding 10 μl of TMT reagent to each sample. Per set, a global internal standard (pool of all cohort samples) was included as the last TMT channel (135N) for reference and normalization. The reaction mixture was incubated for 1 hour under constant agitation, and, afterward, the labeling process was quenched by the addition of hydroxylamine to a final concentration of 0.2% (v/v). After an incubation period of 30 min, the samples were combined into 18-plex sets and subsequently acidified with 0.5 M hydrochloric acid to precipitate DOC as well as diluted with 0.1% trifluoroacetic acid (TFA). To remove DOC, TMT sets were centrifuged at 4000*g* for 15 min at 4°C, and the resulting supernatant was subjected to desalting by solid-phase extraction. Desalting was performed on reversed-phase C18 cartridges (Sep-Pak C18 light) with a vacuum manifold. The columns were first washed twice with 1000 μl of 0.1% TFA in 80% ACN and then equilibrated with two washes of 1000 μl 0.1% TFA. After sample loading, the column was again washed twice with 1000 μl of 0.1% TFA, and, lastly, the peptides were eluted with 0.1% TFA and 80% ACN. The eluate was split into three aliquots of equal volume, dried by vacuum centrifugation, and stored at −20°C. Plasma NfL and other CSF marker measurements are detailed in Supplementary Methods.

Offline high-pH reversed-phase HPLC sample fractionation

Offline high-pH high-performance liquid chromatography (HPLC) fractionation was performed on an UltiMate 3000 Nano LC system. Each TMT set aliquot was dissolved in 22 μl of 2.5 mM NH_4OH, of which 20 μl was injected to be separated on an XBridge BEH C18 column (pore size, 130 Å; inner diameter, 4.6 mm). Peptide elution was accomplished using the following gradient: Buffer B was increased from 1 to 45% over a 65-min period (flow rate of 100 μl/min), whereas buffer C was maintained at 10% (buffer A, H_2O; buffer B, 84% ACN; buffer C, 25 mM NH_4OH). The resulting fractions were collected circling over two rows in a 96-well microtiter plate at 1-min intervals, yielding 24 concatenated fractions. Subsequent column cleaning was performed at 90% B and 10% C for 10 min followed by an equilibration at 1% B and 10% C for 10 min. All fractions were subjected to vacuum centrifugation and stored dry at −20°C until subsequent liquid chromatography–mass spectrometry (LC-MS) analysis.

LC-MS

Fractions were dissolved in 50 μl of 0.05% TFA and 0.1% bovine serum albumin (loading buffer) and loaded on a nano-LC (Ultimate RSLC Nano, Thermo Fisher Scientific) equipped with a C18 trap column (PepMap Acclaim 300 μm by 5 mm, Thermo Fisher Scientific) and C18 separation column (PepMap Acclaim 75 μm by 500 mm, Thermo Fisher Scientific), connected to an Orbitrap Fusion Lumos Tribrid mass spectrometer (Thermo Fisher Scientific), fitted with an Easy Spray Source and a high-field asymmetric waveform ion mobility spectrometry unit for spatial ion separation. Peptides were separated according to the following gradient: 5 min, 4% B; 6 min, 10% B; 74 min, 40% B; 75 min, 100% B (buffer A: 0.1% FA; buffer B: 84% ACN, 0.1% FA). In the positive ion mode, alternating tandem mass spectrometry (MS/MS) cycles (cycle time = 1.5 s) were performed at compensation voltages (CVs) of CV = −70 V, CV = −50 V. A full Orbitrap MS scan was recorded with the parameters specified as follows: R = 120 k, AGC target = 100%, max injection time = 50 ms. The full MS scan was then followed by data-dependent Orbitrap MS/MS scans set to the following parameters: R = 50 k, AGC target = 200%, max. injection time = 120 ms, isolation window = 0.7 m/z; activation type, higher-energy collisional dissociation.

Statistical analysis

All statistical analyses were performed with R version 4.1.2. For basic demographic variables, omnibus Kruskal-Wallis tests were performed for continuous variables, whereas Fisher's exact tests were used for categorical variables. Unless otherwise specified, Spearman correlations were used to test associations between continuous variables. To assess differentially abundant proteins across the diagnostic groups, linear regression models were built with the $\log_2$-transformed value of the measured protein abundance as dependent variable, testing the effect of the diagnostic group and adjusting for both age and sex as covariates. The resulting *P* values were adjusted with the Benjamini-Hochberg procedure to account for multiple testing. Statistical significance (α) was set at a two-sided $P < 0.05$. To ensure a minimum number of observations per group, proteins with a high fraction of missing values (>75% of participants) were excluded from the regression analysis. In addition, groupwise outlier removal of protein measurements (±1.5 × IQR) was performed before regression analysis because the presence of outliers can severely affect the resulting test

Downloaded from https://www.science.org at Universita Degli Studi Di Trento on February 10, 2025

statistics, potentially increasing the rate of false negatives in the initial biomarker discovery phase. For all subsequent statistical analyses as well as box plots shown here, outliers were not removed. Linear models (also adjusted for age and sex), including only one member from each family, were performed in comparisons when more than five participants were available in both groups. To identify mutation-specific signatures, linear models were fitted including protein abundance as a dependent variable while evaluating the effect of each mutation group including affectation (absence/presence of symptoms) as well as age and sex as covariates. To identify subsets of co-correlated proteins relating to pathophysiological features of genetic FTD, we performed network analysis (WGCNA) followed by GO annotation of the output modules. The prognostic properties of protein networks were evaluated using linear mixed effects models. The specifics of each of these methods are described in Supplementary Methods.

Supplementary Materials

The PDF file includes:
Methods
Figs. S1 to S25
References (*53*–*56*)

Other Supplementary Material for this manuscript includes the following:
Tables S1 to S10
MDAR Reproducibility Checklist

REFERENCES AND NOTES

1. C. V. Greaves, J. D. Rohrer, An update on genetic frontotemporal dementia. *J. Neurol.* **266**, 2075–2086 (2019).
2. S. Hendriks, K. Peetoom, C. Bakker, W. M. Van Der Flier, J. M. Papma, R. Koopmans, F. R. J. Verhey, M. De Vugt, S. Köhler, A. Withall, J. L. Parlevliet, Ö. Uysal-Bozkir, R. C. Gibson, S. M. Neita, T. R. Nielsen, L. C. Salem, J. Nyberg, M. A. Lopes, J. C. Dominguez, M. F. De Guzman, A. Egeberg, K. Radford, T. Broe, M. Subramaniam, E. Abdin, A. C. Bruni, R. Di Lorenzo, K. Smith, L. Flicker, M. O. Mol, M. Basta, D. Yu, G. Masika, M. S. Petersen, L. Ruano, Global prevalence of young-onset dementia: A systematic review and meta-analysis. *JAMA Neurol.* **78**, 1080–1090 (2021).
3. I. R. A. Mackenzie, M. Neumann, Molecular neuropathology of frontotemporal dementia: Insights into disease mechanisms from postmortem studies. *J. Neurochem.* **138** (suppl. 1) 54–70 (2016).
4. J. D. Rohrer, R. Guerreiro, J. Vandrovcova, J. Uphill, D. Reiman, J. Beck, A. M. Isaacs, A. Authier, R. Ferrari, N. C. Fox, I. R. A. MacKenzie, J. D. Warren, R. De Silva, J. Holton, T. Revesz, J. Hardy, S. Mead, M. N. Rossor, The heritability and genetics of frontotemporal lobar degeneration. *Neurology* **73**, 1451–1456 (2009).
5. C. H. van Dyck, Anti-amyloid-β monoclonal antibodies for Alzheimer's disease: Pitfalls and promise. *Biol. Psychiatry* **83**, 311–319 (2018).
6. M. R. Al Shweiki, P. Steinacker, P. Oeckl, B. Hengerer, A. Danek, K. Fassbender, J. Diehl-Schmid, H. Jahn, S. Anderl-Straub, A. C. Ludolph, C. Schönfeldt-Lecuona, M. Otto, Neurofilament light chain as a blood biomarker to differentiate psychiatric disorders from behavioural variant frontotemporal dementia. *J. Psychiatr. Res.* **113**, 137–140 (2019).
7. J. C. Rojas, P. Wang, A. M. Staffaroni, C. Heller, Y. Cobigo, A. Wolf, S. Y. M. Goh, P. A. Ljubenkov, H. W. Heuer, J. C. Fong, J. B. Taylor, E. Veras, L. Song, A. Jeromin, D. Hanlon, L. Yu, A. Khinikar, R. Sivasankaran, A. Kieloch, M. A. Valentin, A. M. Karydas, L. L. Mitic, R. Pearlman, J. Kornak, J. H. Kramer, B. L. Miller, K. Kantarci, D. S. Knopman, N. Graff-Radford, L. Petrucelli, R. Rademakers, D. J. Irwin, M. Grossman, E. M. Ramos, G. Coppola, M. F. Mendez, Y. Bordelon, B. C. Dickerson, N. Ghoshal, E. D. Huey, I. R. Mackenzie, B. S. Appleby, K. Domoto-Reilly, G. Y. R. Hsiung, A. W. Toga, S. Weintraub, D. I. Kaufer, D. Kerwin, I. Litvan, C. U. Onyike, A. Pantelyat, E. D. Roberson, M. C. Tartaglia, T. Foroud, W. Chen, J. Czerkowicz, D. L. Graham, J. C. van Swieten, B. Borroni, R. Sanchez-Valle, F. Moreno, R. Laforce, C. Graff, M. Synofzik, D. Galimberti, J. B. Rowe, M. Masellis, E. Finger, R. Vandenberghe, A. de Mendonça, F. Tagliavini, I. Santana, S. Ducharme, C. R. Butler, A. Gerhard, J. Levin, A. Danek, M. Otto, S. Sorbi, D. M. Cash, R. S. Convery, M. Bocchetta, M. Foiani, C. V. Greaves, G. Peakman, L. Russell, I. Swift, E. Todd, J. D. Rohrer, B. F. Boeve, H. J. Rosen, A. L. Boxer, ALLFTD and GENFI consortia, Plasma neurofilament light for prediction of disease progression in familial frontotemporal lobar degeneration. *Neurology* **96**, e2296–e2312 (2021).
8. A. M. Staffaroni, M. Quintana, B. Wendelberger, H. W. Heuer, L. L. Russell, Y. Cobigo, A. Wolf, S. Y. M. Goh, L. Petrucelli, T. F. Gendron, C. Heller, A. L. Clark, J. C. Taylor, A. Wise, E. Ong, L. Forsberg, D. Brushaber, J. C. Rojas, L. VandeVrede, P. Ljubenkov, J. Kramer, K. B. Casaletto, B. Appleby, Y. Bordelon, H. Botha, B. C. Dickerson, K. Domoto-Reilly, J. A. Fields, T. Foroud, R. Gavrilova, D. Geschwind, N. Ghoshal, J. Goldman, J. Graff-Radford, N. Graff-Radford, M. Grossman, M. G. H. Hall, G. Y. Hsiung, E. D. Huey, D. Irwin, D. T. Jones, K. Kantarci, D. Kaufer, D. Knopman, W. Kremers, A. L. Lago, M. I. Lapid, I. Litvan, D. Lucente, I. R. Mackenzie, M. F. Mendez, C. Mester, B. L. Miller, C. U. Onyike, R. Rademakers, V. K. Ramanan, E. M. Ramos, M. Rao, K. Rascovsky, K. P. Rankin, E. D. Roberson, R. Savica, M. C. Tartaglia, S. Weintraub, B. Wong, D. M. Cash, A. Bouzigues, I. J. Swift, G. Peakman, M. Bocchetta, E. G. Todd, R. S. Convery, J. B. Rowe, B. Borroni, D. Galimberti, P. Tiraboschi, M. Masellis, E. Finger, J. C. van Swieten, H. Seelaar, L. C. Jiskoot, S. Sorbi, C. R. Butler, C. Graff, A. Gerhard, T. Langheinrich, R. Laforce, R. Sanchez-Valle, A. de Mendonça, F. Moreno, M. Synofzik, R. Vandenberghe, S. Ducharme, I. Le Ber, J. Levin, A. Danek, M. Otto, F. Pasquier, I. Santana, J. Kornak, B. F. Boeve, H. J. Rosen, J. D. Rohrer, A. L. Boxer, Frontotemporal Dementia Prevention Initiative (FPI) Investigators, Temporal order of clinical and biomarker changes in familial frontotemporal dementia. *Nat. Med.* **28**, 2194–2206 (2022).
9. N. Finch, M. Baker, R. Crook, K. Swanson, K. Kuntz, R. Surtees, G. Bisceglio, A. Rovelet-Lecrux, B. Boeve, R. C. Petersen, D. W. Dickson, S. G. Younkin, V. Deramecourt, J. Crook, N. R. Graff-Radford, R. Rademakers, Plasma progranulin levels predict progranulin mutation status in frontotemporal dementia patients and asymptomatic family members. *Brain* **132** (Pt. 3), 583–591 (2009).
10. L. H. H. Meeter, H. Patzke, G. Loewen, E. G. P. Dopper, Y. A. L. Pijnenburg, R. Van Minkelen, J. C. Van Swieten, Progranulin levels in plasma and cerebrospinal fluid in granulin mutation carriers. *Dement. Geriatr. Cogn. Dis. Extra* **6**, 330–340 (2016).
11. M. Chatterjee, S. Özdemir, C. Fritz, W. Möbius, L. Kleineidam, E. Mandelkow, J. Biernat, C. Doğdu, O. Peters, N. C. Cosma, X. Wang, L. S. Schneider, J. Priller, E. Spruth, A. A. Kühn, P. Krause, T. Klockgether, I. R. Vogt, O. Kimmich, A. Spottke, D. C. Hoffmann, K. Fliessbach, C. Miklitz, C. McCormick, P. Weydt, B. Falkenburger, M. Brandt, R. Guenther, E. Dinter, J. Wiltfang, N. Hansen, M. Bähr, I. Zerr, A. Flöel, P. J. Nestor, E. Düzel, W. Glanz, E. Incesoy, K. Bürger, D. Janowitz, R. Perneczky, B. S. Rauchmann, F. Hopfner, O. Wagemann, J. Levin, S. Teipel, I. Kilimann, D. Goerss, J. Prudlo, T. Gasser, K. Brockmann, D. Mengel, M. Zimmermann, M. Synofzik, C. Wilke, J. Selma-González, J. Turon-Sans, M. A. Santos-Santos, D. Alcolea, S. Rubio-Guerra, J. Fortea, Á. Carbayo, A. Lleó, R. Rojas-García, I. Illán-Gala, M. Wagner, I. Frommann, S. Roeske, L. Bertram, M. T. Heneka, F. Brosseron, A. Ramirez, M. Schmid, R. Beschorner, A. Halle, J. Herms, M. Neumann, N. R. Barthélemy, R. J. Bateman, P. Rizzu, P. Heutink, O. Dols-Icardo, G. Höglinger, A. Hermann, A. Schneider, Plasma extracellular vesicle tau and TDP-43 as diagnostic biomarkers in FTD and ALS. *Nat. Med.* **30**, 1771–1783 (2024).
12. S. Bergström, L. Öijerstedt, J. Remnestål, J. Olofsson, A. Ullgren, H. Seelaar, J. C. van Swieten, M. Synofzik, R. Sanchez-Valle, F. Moreno, E. Finger, M. Masellis, C. Tartaglia, R. Vandenberghe, R. Laforce, D. Galimberti, B. Borroni, C. R. Butler, A. Gerhard, S. Ducharme, J. D. Rohrer, A. Månberg, C. Graff, P. Nilsson, Genetic Frontotemporal Dementia Initiative (GENFI), A panel of CSF proteins separates genetic frontotemporal dementia from presymptomatic mutation carriers: A GENFI study. *Mol. Neurodegener.* **16**, 79 (2021).
13. J. Remnestål, L. Öijerstedt, A. Ullgren, J. Olofsson, S. Bergström, K. Kultima, M. Ingelsson, L. Kilander, M. Uhlén, A. Månberg, C. Graff, P. Nilsson, Altered levels of CSF proteins in patients with FTD, presymptomatic mutation carriers and non-carriers. *Transl. Neurodegener.* **9**, 27 (2020).
14. C. E. Teunissen, N. Elias, M. J. A. Koel-Simmelink, S. Durieux-Lu, A. Malekzadeh, T. V. Pham, S. R. Piersma, T. Beccari, L. H. H. Meeter, E. G. P. Dopper, J. C. van Swieten, C. R. Jimenez, Y. A. L. Pijnenburg, Novel diagnostic cerebrospinal fluid biomarkers for pathologic subtypes of frontotemporal dementia identified by proteomics. *Alzheimers Dement.* **2**, 86–94 (2016).
15. E. L. van der Ende, L. H. Meeter, C. Stingl, J. G. J. van Rooij, M. P. Stoop, D. A. T. Nijholt, R. Sanchez-Valle, C. Graff, L. Öijerstedt, M. Grossman, C. McMillan, Y. A. L. Pijnenburg, R. Laforce, G. Binetti, L. Benussi, R. Ghidoni, T. M. Luider, H. Seelaar, J. C. van Swieten, Novel CSF biomarkers in genetic frontotemporal dementia identified by proteomics. *Ann. Clin. Transl. Neurol.* **6**, 698–707 (2019).
16. N. Mattsson, U. Rüetschi, Y. A. L. Pijnenburg, M. A. Blankenstein, V. N. Podust, S. Li, I. Fagerberg, L. Rosengren, K. Blennow, H. Zetterberg, Novel cerebrospinal fluid biomarkers of axonal degeneration in frontotemporal dementia. *Mol. Med. Rep.* **1**, 757–761 (2008).
17. P. Barschke, P. Oeckl, P. Steinacker, M. H. D. R. Al Shweiki, J. H. Weishaupt, G. B. Landwehrmeyer, S. Anderl-Straub, P. Weydt, J. Diehl-Schmid, A. Danek, J. Kornhuber, M. L. Schroeter, J. Prudlo, H. Jahn, K. Fassbender, M. Lauer, E. L. Van Der Ende, J. C. Van Swieten, A. E. Volk, A. C. Ludolph, M. Otto, German FTLD consortium, Different CSF protein profiles in amyotrophic lateral sclerosis and frontotemporal dementia with

Downloaded from https://www.science.org at Universita Degli Studi Di Trento on February 10, 2025

C9orf72 hexanucleotide repeat expansion. *J. Neurol. Neurosurg. Psychiatry* **91**, 503–511 (2020).
18. J. Nilsson, J. Gobom, S. Sjödin, G. Brinkmalm, N. J. Ashton, J. Svensson, P. Johansson, E. Portelius, H. Zetterberg, K. Blennow, A. Brinkmalm, Cerebrospinal fluid biomarker panel for synaptic dysfunction in Alzheimer's disease. *Alzheimers Dement.* **13**, e12179 (2021).
19. F. Llorens, K. Thüne, W. Tahir, E. Kanata, D. Diaz-Lucena, K. Xanthopoulos, E. Kovatsi, C. Pleschka, P. Garcia-Esparcia, M. Schmitz, D. Ozbay, S. Correia, Â. Correia, I. Milosevic, O. Andréoletti, N. Fernández-Borges, I. M. Vorberg, M. Glatzel, T. Sklaviadis, J. M. Torres, S. Krasemann, R. Sánchez-Valle, I. Ferrer, I. Zerr, YKL-40 in the brain and cerebrospinal fluid of neurodegenerative dementias. *Mol. Neurodegener.* **12**, 83 (2017).
20. P. Oeckl, P. Weydt, D. R. Thal, J. H. Weishaupt, A. C. Ludolph, M. Otto, Proteomics in cerebrospinal fluid and spinal cord suggests UCHL1, MAP2 and GPNMB as biomarkers and underpins importance of transcriptional pathways in amyotrophic lateral sclerosis. *Acta Neuropathol.* **139**, 119–134 (2020).
21. G. Ary, H. Sich, C. Larence, J. G. Ibbs, E. H. L. Ee, G. H. Arrington, The 14-3-3 brain protein in cerebrospinal fluid as a marker for transmissible spongiform encephalopathies. *N. Engl. J. Med.* **335**, 924–930 (1996).
22. S. Palmqvist, S. Janelidze, Y. T. Quiroz, H. Zetterberg, F. Lopera, E. Stomrud, Y. Su, Y. Chen, G. E. Serrano, A. Leuzy, N. Mattsson-Carlgren, O. Strandberg, R. Smith, A. Villegas, D. Sepulveda-Falla, X. Chai, N. K. Proctor, T. G. Beach, K. Blennow, J. L. Dage, E. M. Reiman, O. Hansson, Discriminative accuracy of plasma phospho-tau217 for Alzheimer sisease vs other neurodegenerative disorders. *JAMA* **324**, 772–781 (2020).
23. N. K. Magdalinou, A. J. Noyce, R. Pinto, E. Lindstrom, J. Holmén-Larsson, M. Holtta, K. Blennow, H. R. Morris, T. Skillbäck, T. T. Warner, A. J. Lees, I. Pike, M. Ward, H. Zetterberg, J. Gobom, Identification of candidate cerebrospinal fluid biomarkers in parkinsonism using quantitative proteomics. *Parkinsonism Relat. Disord.* **37**, 65–71 (2017).
24. S. Weiner, M. Sauer, P. J. Visser, B. M. Tijms, E. Vorontsov, K. Blennow, H. Zetterberg, J. Gobom, Optimized sample preparation and data analysis for TMT proteomic analysis of cerebrospinal fluid applied to the identification of Alzheimer's disease biomarkers. *Clin. Proteomics* **19**, 13 (2022).
25. B. M. Tijms, J. Gobom, L. Reus, I. Jansen, S. Hong, V. Dobricic, F. Kilpert, M. Ten Kate, F. Barkhof, M. Tsolaki, F. R. J. Verhey, J. Popp, P. Martinez-Lage, R. Vandenberghe, A. Lleó, J. L. Molinuevo, S. Engelborghs, L. Bertram, S. Lovestone, J. Streffer, S. Vos, I. Bos, Alzheimer's Disease Neuroimaging Initiative (ADNI), K. Blennow, P. Scheltens, C. E. Teunissen, H. Zetterberg, P. J. Visser, Pathophysiological subtypes of Alzheimer's disease based on cerebrospinal fluid proteomics. *Brain* **143**, 3776–3792 (2020).
26. A. Sogorb-Esteve, J. Nilsson, I. J. Swift, C. Heller, M. Bocchetta, L. L. Russell, G. Peakman, R. S. Convery, J. C. van Swieten, H. Seelaar, B. Borroni, D. Galimberti, R. Sanchez-Valle, R. Laforce, F. Moreno, M. Synofzik, C. Graff, M. Masellis, M. C. Tartaglia, J. B. Rowe, R. Vandenberghe, E. Finger, F. Tagliavini, I. Santana, C. R. Butler, S. Ducharme, A. Gerhard, A. Danek, J. Levin, M. Otto, S. Sorbi, I. Le Ber, F. Pasquier, J. Gobom, A. Brinkmalm, K. Blennow, H. Zetterberg, J. D. Rohrer, GENetic FTD Initiative, Differential impairment of cerebrospinal fluid synaptic biomarkers in the genetic forms of frontotemporal dementia. *Alzheimers. Res. Ther.* **14**, 118 (2022).
27. I. Pesämaa, S. A. Müller, S. Robinson, A. Darcher, D. Paquet, H. Zetterberg, S. F. Lichtenthaler, C. Haass, A microglial activity state biomarker panel differentiates FTD-granulin and Alzheimer's disease patients from controls. *Mol. Neurodegener.* **18**, 70 (2023).
28. L. Higginbotham, L. Ping, E. B. Dammer, D. M. Duong, M. Zhou, M. Gearing, C. Hurst, J. D. Glass, S. A. Factor, E. C. B. Johnson, I. Hajjar, J. J. Lah, A. I. Levey, N. T. Seyfried, Integrated proteomics reveals brain-based cerebrospinal fluid biomarkers in asymptomatic and symptomatic Alzheimer's disease. *Sci. Adv.* **6**, eaaz9360 (2020).
29. E. Portelius, B. Olsson, K. Höglund, N. C. Cullen, H. Kvartsberg, U. Andreasson, H. Zetterberg, Å. Sandelius, L. M. Shaw, V. M. Y. Lee, D. J. Irwin, M. Grossman, D. Weintraub, A. Chen-Plotkin, D. A. Wolk, L. McCluskey, L. Elman, J. McBride, J. B. Toledo, J. Q. Trojanowski, K. Blennow, Cerebrospinal fluid neurogranin concentration in neurodegeneration: Relation to clinical phenotypes and neuropathology. *Acta Neuropathol.* **136**, 363–376 (2018).
30. N. J. Ashton, S. Janelidze, A. Al Khleifat, A. Leuzy, E. L. van der Ende, T. K. Karikari, A. L. Benedet, T. A. Pascoal, A. Lleó, L. Parnetti, D. Galimberti, L. Bonanni, A. Pilotto, A. Padovani, J. Lycke, L. Novakova, M. Axelsson, L. Velayudhan, G. D. Rabinovici, B. Miller, C. Pariante, N. Nikkheslat, S. M. Resnick, M. Thambisetty, M. Schöll, G. Fernández-Eulate, F. J. Gil-Bea, A. López de Munain, A. Al-Chalabi, P. Rosa-Neto, A. Strydom, P. Svenningsson, E. Stomrud, A. Santillo, D. Aarsland, J. C. van Swieten, S. Palmqvist, H. Zetterberg, K. Blennow, A. Hye, O. Hansson, A multicentre validation study of the diagnostic value of plasma neurofilament light. *Nat. Commun.* **12**, 3400 (2021).
31. I. Illán-Gala, D. Alcolea, V. Montal, O. Dols-Icardo, L. Muñoz, N. de Luna, J. Turón-Sans, E. Cortés-Vicente, M. B. Sánchez-Saudinós, A. Subirana, I. Sala, R. Blesa, J. Clarimón, J. Fortea, R. Rojas-García, A. Lleó, CSF sAPPβ, YKL-40, and NfL along the ALS-FTD spectrum. *Neurology* **91**, e1619–e1628 (2018).
32. E. L. Van Der Ende, M. Xiao, D. Xu, J. M. Poos, J. L. Panman, L. C. Jiskoot, L. H. Meeter, E. G. P. Dopper, J. M. Papma, C. Heller, R. Convery, K. Moore, M. Bocchetta, M. Neason, G. Peakman, D. M. Cash, C. E. Teunissen, C. Graff, M. Synofzik, F. Moreno, E. Finger, R. Sánchez-Valle, R. Vandenberghe, R. Laforce, M. Masellis, M. C. Tartaglia, J. B. Rowe, C. R. Butler, S. Ducharme, A. Gerhard, A. Danek, J. Levin, Y. A. L. Pijnenburg, M. Otto, B. Borroni, F. Tagliavini, A. De Mendonca, I. Santana, D. Galimberti, H. Seelaar, J. D. Rohrer, P. F. Worley, J. C. Van Swieten, Genetic Frontotemporal Dementia Initiative (GENFI), Neuronal pentraxin 2: A synapse-derived CSF biomarker in genetic frontotemporal dementia. *J. Neurol. Neurosurg. Psychiatry* **91**, 612–621 (2020).
33. J. Nilsson, J. Constantinescu, B. Nellgård, P. Jakobsson, W. S. Brum, J. Gobom, L. Forsgren, K. Dalla, R. Constantinescu, H. Zetterberg, O. Hansson, K. Blennow, D. Bäckström, A. Brinkmalm, Cerebrospinal fluid biomarkers of synaptic dysfunction are altered in Parkinson's disease and related disorders. *Mov. Disord.* **38**, 267–277 (2023).
34. E. C. B. Johnson, E. B. Dammer, D. M. Duong, L. Ping, M. Zhou, L. Yin, L. A. Higginbotham, A. Guajardo, B. White, J. C. Troncoso, M. Thambisetty, T. J. Montine, E. B. Lee, J. Q. Trojanowski, T. G. Beach, E. M. Reiman, V. Haroutunian, M. Wang, E. Schadt, B. Zhang, D. W. Dickson, N. Ertekin-Taner, T. E. Golde, V. A. Petyuk, P. L. De Jager, D. A. Bennett, T. S. Wingo, S. Rangaraju, I. Hajjar, J. M. Shulman, J. J. Lah, A. I. Levey, N. T. Seyfried, Large-scale proteomic analysis of Alzheimer's disease brain and cerebrospinal fluid reveals early changes in energy metabolism associated with microglia and astrocyte activation. *Nat. Med.* **26**, 769–780 (2020).
35. S. Rangaraju, E. B. Dammer, S. A. Raza, P. Rathakrishnan, H. Xiao, T. Gao, D. M. Duong, M. W. Pennington, J. J. Lah, N. T. Seyfried, A. I. Levey, Identification and therapeutic modulation of a pro-inflammatory subset of disease-associated-microglia in Alzheimer's disease. *Mol. Neurodegener.* **13**, 24 (2018).
36. C. J. Garwood, L. E. Ratcliffe, J. E. Simpson, P. R. Heath, P. G. Ince, S. B. Wharton, Review: Astrocytes in Alzheimer's disease and other age-associated dementias: A supporting player with a central role. *Neuropathol. Appl. Neurobiol.* **43**, 281–298 (2017).
37. M. Huang, E. Modeste, E. Dammer, P. Merino, G. Taylor, D. M. Duong, Q. Deng, C. J. Holler, M. Gearing, D. Dickson, N. T. Seyfried, T. Kukar, Network analysis of the progranulin-deficient mouse brain proteome reveals pathogenic mechanisms shared in human frontotemporal dementia caused by GRN mutations. *Acta Neuropathol. Commun.* **8**, 163 (2020).
38. S. Oh, Y. Jang, C. H. Na, Discovery of biomarkers for amyotrophic lateral sclerosis from human cerebrospinal fluid using mass-spectrometry-based proteomics. *Biomedicine* **11**, 1250 (2023).
39. R. Mao, Y. Wang, F. Wang, L. Zhou, S. Yan, S. Lu, W. Shi, Y. Zhang, Identification of four biomarkers of human skin aging by comprehensive single cell transcriptome, transcriptome, and proteomics. *Front. Genet.* **13**, 881051 (2022).
40. K. Kawane, H. Fukuyama, G. Kondoh, J. Takeda, Y. Ohsawa, Y. Uchiyama, S. Nagata, Requirement of DNase II for definitive erythropoiesis in the mouse fetal liver. *Science* **292**, 1546–1549 (2001).
41. H. D. Shin, B. L. Park, H. S. Cheong, H. S. Lee, J. B. Jun, S. C. Bae, DNase II polymorphisms associated with risk of renal disorder among systemic lupus erythematosus patients. *J. Hum. Genet.* **50**, 107–111 (2005).
42. P. A. Keyel, Dnases in health and disease. *Dev. Biol.* **429**, 1–11 (2017).
43. J. Root, P. Merino, A. Nuckols, M. Johnson, T. Kukar, Lysosome dysfunction as a cause of neurodegenerative diseases: Lessons from frontotemporal dementia and amyotrophic lateral sclerosis. *Neurobiol. Dis.* **154**, 105360 (2021).
44. C. J. Holler, G. Taylor, Q. Deng, T. Kukar, Intracellular proteolysis of progranulin generates stable, lysosomal granulins that are haploinsufficient in patients with frontotemporal dementia caused by *GRN* mutations. *eNeuro* **4**, ENEURO.0100-17.2017 (2017).
45. M. Hutton, C. L. Lendon, P. Rizzu, M. Baker, S. Froelich, H. Houlden, S. Pickering-Brown, S. Chakraverty, A. Isaacs, A. Grover, J. Hackett, J. Adamson, S. Lincoln, D. Dickson, P. Davies, R. C. Petersen, M. Stevens, E. de Graaff, E. Wauters, J. van Baren, M. Hillebrand, M. Joosse, J. M. Kwon, P. Nowotny, L. K. Che, J. Norton, J. C. Morris, L. A. Reed, J. Trojanowski, H. Basun, L. Lannfelt, M. Neystat, S. Fahn, F. Dark, T. Tannenberg, P. R. Dodd, N. Hayward, J. B. Kwok, P. R. Schofield, A. Andreadis, J. Snowden, D. Craufurd, D. Neary, F. Owen, B. A. Oostra, J. Hardy, A. Goate, J. van Swieten, D. Mann, T. Lynch, P. Heutink, Association of missense and 5′-splice-site mutations in tau with the inherited dementia FTDP-17. *Nature* **393**, 702–705 (1998).
46. F. Lim, F. Hernández, J. J. Lucas, P. Gómez-Ramos, M. A. Morán, J. Ávila, FTDP-17 mutations in tau transgenic mice provoke lysosomal abnormalities and Tau filaments in forebrain. *Mol. Cell. Neurosci.* **18**, 702–714 (2001).
47. C. D. Pacheco, M. J. Elrick, A. P. Lieberman, Tau normal function influences Niemann-Pick type C disease pathogenesis in mice and modulates autophagy in NPC1-deficient cells. *Autophagy* **5**, 548–550 (2009).
48. N. Ashtari, X. Jiao, M. Rahimi-Balaei, S. Amiri, S. E. Mehr, B. Yeganeh, H. Marzban, Lysosomal acid phosphatase biosynthesis and dysfunction: A mini review focused on lysosomal enzyme dysfunction in brain. *Curr. Mol. Med.* **16**, 439–446 (2016).
49. Q. Zhang, Y. Meng, L. Zhang, J. Chen, D. Zhu, RNF13: A novel RING-type ubiquitin ligase over-expressed in pancreatic cancer. *Cell Res.* **19**, 348–357 (2009).
50. J. M. Berg, J. L. Tymoczko, L. Stryer, *Biochemistry* (Freeman W. H. and Company, ed. 5, 2002).
51. M. L. Gorno-Tempini, A. E. Hillis, S. Weintraub, A. Kertesz, M. Mendez, S. F. Cappa, J. M. Ogar, J. D. Rohrer, S. Black, B. F. Boeve, F. Manes, N. F. Dronkers, R. Vandenberghe,

Downloaded from https://www.science.org at Universita Degli Studi Di Trento on February 10, 2025

K. Rascovsky, K. Patterson, B. L. Miller, D. S. Knopman, J. R. Hodges, M. M. Mesulam, M. Grossman, Classification of primary progressive aphasia and its variants. *Neurology* **76**, 1006–1014 (2011).
52. K. Rascovsky, J. R. Hodges, D. Knopman, M. F. Mendez, J. H. Kramer, J. Neuhaus, J. C. Van Swieten, H. Seelaar, E. G. P. Dopper, C. U. Onyike, A. E. Hillis, K. A. Josephs, B. F. Boeve, A. Kertesz, W. W. Seeley, K. P. Rankin, J. K. Johnson, M. L. Gorno-Tempini, H. Rosen, C. E. Prioleau-Latham, A. Lee, C. M. Kipps, P. Lillo, O. Piguet, J. D. Rohrer, M. N. Rossor, J. D. Warren, N. C. Fox, D. Galasko, D. P. Salmon, S. E. Black, M. Mesulam, S. Weintraub, B. C. Dickerson, J. Diehl-Schmid, F. Pasquier, V. Deramecourt, F. Lebert, Y. Pijnenburg, T. W. Chow, F. Manes, J. Grafman, S. F. Cappa, M. Freedman, M. Grossman, B. L. Miller, Sensitivity of revised diagnostic criteria for the behavioural variant of frontotemporal dementia. *Brain* **134** (Pt. 9), 2456–2477 (2011).
53. M. J. Cardoso, R. Wolz, M. Modat, N. C. Fox, D. Rueckert, S. Ourselin, Geodesic information flows. *Med. Image Comput. Comput. Assist. Interv.* **15**, 262–270 (2012).
54. I. B. Malone, K. K. Leung, S. Clegg, J. Barnes, J. L. Whitwell, J. Ashburner, N. C. Fox, G. R. Ridgway, Accurate automatic estimation of total intracranial volume: A nuisance variable with less nuisance. *Neuroimage* **104**, 366–372 (2015).
55. P. Langfelder, S. Horvath, WGCNA: An R package for weighted correlation network analysis. *BMC Bioinformatics* **9**, 599 (2008).
56. U. Raudvere, L. Kolberg, I. Kuzmin, T. Arak, P. Adler, H. Peterson, J. Vilo, g:Profiler: A web server for functional enrichment analysis and conversions of gene lists (2019 update). *Nucleic Acids Res.* **47**, W191–W198 (2019).

Acknowledgments: We thank I. Pesämaa for discussions around the work with microglial activation–dependent markers, from which the published results were used as an external validation cohort of this study. **Funding:** This work was supported by a Race Against Dementia fellowship, supported by Alzheimer's Research UK (ARUK-RADF2021A-003 to A.S.-E.) and the UK Dementia Research Institute, which receives its funding from DRI Ltd, funded by the UK Medical Research Council, Alzheimer's Society and Alzheimer's Research UK (to A.S.-E.). The Dementia Research Centre is supported by Alzheimer's Research UK, Alzheimer's Society, Brain Research UK, and the Wolfson Foundation. Coauthors of the manuscript were supported by the Gothenburg Medical Society (Göteborgs Läkaresällskap, #GLS-988641 to J.S.). H.Z. is a Wallenberg scholar and a distinguished professor at the Swedish Research Council supported by grants from the Swedish Research Council (#2023-00356, #2022-01018, and #2019-02397); the European Union's Horizon Europe research and innovation programme under grant agreement no. 101053962; Swedish State Support for Clinical Research (#ALFGBG-71320); the Alzheimer Drug Discovery Foundation (ADDF), USA (#201809-2016862); the AD Strategic Fund and the Alzheimer's Association (#ADSF-21-831376-C, #ADSF-21-831381-C, #ADSF-21-831377-C, and #ADSF-24-1284328-C); the European Partnership on Metrology, cofinanced from the European Union's Horizon Europe Research and Innovation Programme and by the participating states (NEuroBioStand, #22HLT07); the Bluefield Project; Cure Alzheimer's Fund; the Olav Thon Foundation; the Erling-Persson Family Foundation; Familjen Rönströms Stiftelse; Stiftelsen för Gamla Tjänarinnor, Hjärnfonden, Sweden (#FO2022-0270); the European Union's Horizon 2020 research and innovation programme under the Marie Skłodowska-Curie grant agreement no. 860197 (MIRIADE); the European Union Joint Programme—Neurodegenerative Disease Research (JPND2021-00694); the National Institute for Health and Care Research University College London Hospitals Biomedical Research Centre; and the UK Dementia Research Institute at UCL (UKDRI-1003). K.B. is supported by the Swedish Research Council (#2017-00915 and #2022-00732); the Swedish Alzheimer Foundation (#AF-930351, #AF-939721, and #AF-968270); Hjärnfonden, Sweden (#FO2017-0243 and #ALZ2022-0006); the Swedish state under the agreement between the Swedish government and the County Councils, the ALF-agreement (#ALFGBG-715986 and #ALFGBG-965240); the European Union Joint Program for Neurodegenerative Disorders (JPND2019-466-236); the Alzheimer's Association 2021 Zenith Award (ZEN-21-848495); and the Alzheimer's Association 2022-2025 grant (SG-23-1038904 QC). J.C.V.S. was supported by the Dioraphte Foundation grant 09-02-03-00, Association for Frontotemporal Dementias Research Grant 2009, Netherlands Organization for Scientific Research grant HCMI 056-13-018, ZonMw Memorabel (Deltaplan Dementie, project number 733 051 042), Alzheimer Nederland, and the Bluefield Project. F.M. received funding from the Tau Consortium and the Center for Networked Biomedical Research on Neurodegenerative Disease. R.S.-V. is supported by Alzheimer's Research UK Clinical Research Training Fellowship (ARUK-CRF2017B-2) and has received funding from Fundació Marató de TV3, Spain (grant no. 20143810). D.G. received support from the EU Joint Programme–Neurodegenerative Disease Research and the Italian Ministry of Health (PreFrontALS) grant 733051042. C.G. received funding from EU Joint Programme–Neurodegenerative Disease Research-Prefrontals VR Dnr 529-2014-7504, VR 2015-02926, and 2018-02754; the Swedish FTD Inititative-Schörling Foundation; Alzheimer Foundation; Brain Foundation; and Stockholm County Council ALF. M.M. has received funding from a Canadian Institute of Health Research operating grant and the Weston Brain Institute and Ontario Brain Institute. J.B.R. has received funding from the Wellcome Trust (220258) and the Bluefield Project and is supported by the Cambridge University Centre for Frontotemporal Dementia, the Medical Research Council (MC_UU_00030/14; MR/T033371/1), and the National Institute for Health Research Cambridge Biomedical Research Centre (NIHR203312). E.F. has received funding from a Canadian Institute of Health Research grant #327387. RV has received funding from the Mady Browaeys Fund for Research into Frontotemporal Dementia. J.L. received funding for this work by the Deutsche Forschungsgemeinschaft German Research Foundation under Germany's Excellence Strategy within the framework of the Munich Cluster for Systems Neurology (EXC 2145 SyNergy—ID 390857198). M.O. has received funding from Germany's Federal Ministry of Education and Research (BMBF). J.D.R. is supported by the Bluefield Project and the National Institute for Health and Care Research University College London Hospitals Biomedical Research Centre and has received funding from an MRC Clinician Scientist Fellowship (MR/M008525/1) and a Miriam Marks Brain Research UK Senior Fellowship. J.G. is supported by Alzheimerfonden (AF-980746) and Stiftelsen för Gamla tjänarinnor (2022-01324). Several authors of this publication are members of the European Reference Network for Rare Neurological Diseases (ERN-RND) - Project ID no. 739510 to J.C.V.S., M.S., R.S.V., A.d.M., M.O., R.V., and J.D.R. This work was also supported by the EU Joint Programme—Neurodegenerative Disease Research GENFI-PROX grant (2019-02248, to J.D.R., M.O., B.B., C.G., J.C.V.S., and M.S.) and by the Clinician Scientist programme "PRECISE.net" funded by the Else Kröner-Fresenius-Stiftung (to M.S.).
Author contributions: A.S.-E., J.D.R., and J.G. designed the study. S.W., A.S.-E., and J.S. performed experiments. J.G. supervised the analytical study. S.W. analyzed the data. A.S.-E. and J.S. assisted with data analyses as well as visualization. A.S.-E., S.W., and J.S. wrote the manuscript. J.G., J.D.R., K.B., and H.Z. revised the manuscript and contributed to data interpretation. All authors read and approved the final manuscript. **Competing interests:** H.Z. has served on scientific advisory boards and as a consultant for Abbvie, Acumen, Alector, Alzinova, ALZPath, Amylyx, Annexon, Apellis, Artery Therapeutics, AZTherapies, Cognito Therapeutics, CogRx, Denali, Eisai, LabCorp, Merry Life, Nervgen, Novo Nordisk, Optoceutics, Passage Bio, Pinteon Therapeutics, Prothena, Red Abbey Labs, reMYND, Roche, Samumed, Siemens Healthineers, Triplet Therapeutics, and Wave; has given lectures in symposia sponsored by Alzecure, Biogen, Cellectricon, Fujirebio, Lilly, Novo Nordisk, and Roche; and is a cofounder of Brain Biomarker Solutions in Gothenburg AB (BBS), which is a part of the GU Ventures Incubator Program (outside submitted work). K.B. has served as a consultant and on advisory boards for Acumen, ALZPath, BioArctic, Biogen, Eisai, Lilly, Moleac Pte. Ltd., Novartis, Ono Pharma, Prothena, Roche Diagnostics, and Siemens Healthineers; has served on data monitoring committees for Julius Clinical and Novartis; has given lectures, produced educational materials, and participated in educational programs for AC Immune, Biogen, Celdara Medical, Eisai, and Roche Diagnostics; and is a cofounder of Brain Biomarker Solutions in Gothenburg AB (BBS), which is a part of the GU Ventures Incubator Program, outside the work presented here. M.S. has received consultancy honoraria from Ionis, UCB, Prevail, Orphazyme, Biogen, Servier, Reata, GenOrph, AviadoBio, Biohaven, Zevra, Lilly, and Solaxa, all unrelated to the present manuscript. J.B.R. has provided consultancy or advisory board input to Alector, Asceneuron, Astronautx, Astex, CumulusNeuro, Cerevance, Clinical Ink, Curasen, Eisai, and Wave, unrelated to the current work. S.D. has provided paid consultancy to QuRALIS, Eisai, and Eli Lilly and has received speaker fees from Eisai. S.D. is an SDMB member of Aviado Bio and IntelGenX. R.V.'s institution has a clinical trial agreement (R.V. as PI) with Alector, AviadioBio, Denali, Eli Lilly, J&J, and UCB. R.V.'s institution has a consultancy agreement (R.V. as DSMB chair) with AC Immune. L.L.R. is a consultant for Prevail Therapeutics. **Data and materials availability:** All data associated with this study are present in the paper or the Supplementary Materials. Proteomic data underlying the results of this study have been deposited in the Dryad repository (DOI: 10.5061/dryad.r7sqv9snk). Individual identifiers have not been included to protect the privacy of study participants but can be requested from the authors. No custom code was used for data analysis; respective R packages have been indicated where applicable. The data used for external validation of the *GRN* results as well as for AD-FTD comparisons are publicly available in the supplementary sections of the respective publications by Pesämaa *et al.*, Tijms *et al.*, and Higginbotham *et al.* This research was funded in whole or in part by the Wellcome Trust [grant number 220258], a cOAlition S organization. The authors will make the author-accepted manuscript (AAM) version available under a CC BY public copyright license.

GENFI authors: In addition to members of GENFI who are coauthors, the following members are collaborators who have contributed to the study design, the recruitment of participants, and the processing of samples at their sites, sending the samples and providing corresponding demographic data of their participants, data analysis, and interpretation: David L. Thomas[2], Thomas Cope[41], Timothy Rittman[41], Alberto Benussi[46], Enrico Premi[47], Roberto Gasparotti[46], Silvana Archetti[47], Stefano Gazzina[47], Valentina Cantoni[46], Andrea Arighi[10,11], Chiara Fenoglio[10,11], Elio Scarpini[10,11], Giorgio Fumagalli[10,11], Vittoria Borracci[10,11], Giacomina Rossi[16], Giorgio Giaccone[16], Giuseppe Di Fede[16], Paola Caroppo[16], Pietro Tiraboschi[16], Sara Prioni[16], Veronica Radaaelli[16], David Tang-Wai[54], Ekaterina Rogaeva[39], Michel Castelo-Branco[17], Morris Freedman[55], Ron Keren[54], Sandra Black[40], Sara Mitchell[40], Christen Shoesmith[38], Robart Bartha[56,57], Rosa Rademakers[58], Jackie Poos[5], Janne M. Papma[5], Lucia Giannini[5], Rick van Minkelen[59], Yolande Pijnenburg[60], Benedetta Nacmias[61], Camilla Ferrari[61], Cristina Polito[62], Gemma Lombardi[61], Valentina Bessi[61], Michele Veldsman[33], Christin Andersson[63], Hakan Thonberg[8], Linn Öijerstedt[8,9], Vesna Jelic[64], Paul Thompson[19], Tobias Langheinrich[19,65], Albert Lladó[6], Anna Antonell[6], Jaume Olives[6], Mircea Balasa[6], Nuria Bargalló[66], Sergi Borrego-Écija[6], Ana Verdelho[67], Carolina Maruta[68], Catarina B. Ferreira[69], Gabriel Miltenberger[15],

Downloaded from https://www.science.org at Universita Degli Studi Di Trento on February 10, 2025

Frederico Simões do Couto[70], Alazne Gabilondo[44,45], Jorge Villanua[71], Marta Cañada[72], Mikel Tainta[45], Miren Zulaica[45], Myriam Barandiaran[44,45], Patricia Alves[45,73], Benjamin Bender[74], Carlo Wilke[42,43], Lisa Graf[42], Annick Vogels[75], Mathieu Vandenbulcke[76,77], Philip van Damme[13,78], Rose Buffaerts[79,80], Koen Poesen[81], Pedro Rosa- Neto[82], Serge Gauthier[83], Agnès Camuzat[35], Alexis Brice[35,36], Anne Bertrand[35,84,85], Aurélie Funkiewiez[35,36], Daisy Rinaldi[35,36], Dario Saracino[35,36], Olivier Colliot[35,84], Sabrina Sayah[35], Catharina Prix[21], Elisabeth Wlasich[21], Olivia Wagemann[21], Sandra Loosli[21], Sonja Schönecker[21], Tobias Hoegen[21], Jolina Lombardi[26], Sarah Anderl-Straub[26], Adeline Rollin[30], Gregory Kuchcinski[28,30], Maxime Bertoux[29,30], Thibaud Lebouvier[28,29,30], Vincent Deramecourt[28,29,30], Beatriz Santiago[17], Diana Duro[17], Maria João Leitão[18], Maria Rosario Almeida[17], Miguel Tábuas-Pereira[17], Sónia Afonso[86].

Affiliations of GENFI authors: Affiliations 1 to 53 can be found on the first page of the paper.

[54]University Health Network, Krembil Research Institute, M5T 0S8, Toronto, Canada. [55]Baycrest Health Sciences, Rotman Research Institute, University of Toronto, M5S 3E6, Toronto, Canada.

[56]Department of Medical Biophysics, University of Western Ontario, N6A 5C1, London, Ontario, Canada. [57]Centre for Functional and Metabolic Mapping, Robarts Research Institute, University of Western Ontario, N6A 5B7, London, Ontario, Canada. [58]Center for Molecular Neurology, University of Antwerp, 2650, Edegem, Belgium. [59]Department of Clinical Genetics, Erasmus Medical Center, 3000, Rotterdam, Netherlands. [60]Amsterdam University Medical Centre, Amsterdam VUmc, 1081 HV, Amsterdam, Netherlands. [61]Department of Neuroscience, Psychology, Drug Research and Child Health, University of Florence, 50139, Florence, Italy.

[62]Department of Biomedical, Experimental and Clinical Sciences "Mario Serio", Nuclear Medicine Unit, University of Florence, 50139, Florence, Italy. [63]Department of Clinical Neuroscience, Karolinska Institutet, Stockholm, 171 65, Solna, Sweden. [64]Division of Clinical Geriatrics, Karolinska Institutet, Stockholm, 171 65, Solna, Sweden. [65]Manchester Centre for Clinical Neurosciences, Department of Neurology, Salford Royal NHS Foundation Trust, M6 8HD, Manchester, UK. [66]Imaging Diagnostic Center, Hospital Clínic, 08036, Barcelona, Spain.

[67]Department of Neurosciences and Mental Health, Centro Hospitalar Lisboa Norte - Hospital de Santa Maria & Faculty of Medicine, University of Lisbon, 1649-028, Lisbon, Portugal.

[68]Laboratory of Language Research, Centro de Estudos Egas Moniz, Faculty of Medicine, University of Lisbon, 2829 – 511, Lisbon, Portugal. [69]Laboratory of Neurosciences, Faculty of Medicine, University of Lisbon, 1649-028, Lisbon, Portugal. [70]Faculdade de Medicina, Universidade Católica Portuguesa, 2635-631, Rio de Mouro, Portugal. [71]OSATEK, University of Donostia, San Sebastian, 20014, Gipuzkoa, Spain. [72]CITA Alzheimer, San Sebastian, 20009, Gipuzkoa, Spain. [73]Department of Educational Psychology and Psychobiology, Faculty of Education, International University of La Rioja, 26006, Logroño, Spain. [74]Department of Diagnostic and Interventional Neuroradiology, University of Tübingen, 72074, Tübingen. [75]Department of Human Genetics, KU Leuven, 3000, Leuven, Belgium. [76]Geriatric Psychiatry Service, University Hospitals Leuven, 3000, Leuven, Belgium. [77]Neuropsychiatry, Department of Neurosciences, KU Leuven, 3000, Leuven, Belgium. [78]Laboratory for Neurobiology, VIB-KU Leuven Centre for Brain Research, 3000, Leuven, Belgium. [79]Department of Biomedical Sciences, University of Antwerp, 2000, Antwerp, Belgium. [80]Biomedical Research Institute, Hasselt University, 3500 Hasselt, Belgium. [81]Laboratory for Molecular Neurobiomarker Research, KU Leuven, 3000, Leuven, Belgium. [82]Translational Neuroimaging Laboratory, McGill Centre for Studies in Aging, McGill University, H3A 2B4, Montreal, Québec, Canada. [83]Alzheimer Disease Research Unit, McGill Centre for Studies in Aging, Department of Neurology & Neurosurgery, McGill University, H4H 1R2, Montreal, Québec, Canada. [84]Inria, Aramis project-team, 75013, Paris, France. [85]Centre pour l'Acquisition et le Traitement des Images, Institut du Cerveau et la Moelle, 75013, Paris, France. [86]Instituto Ciencias Nucleares Aplicadas a Saude, Universidade de Coimbra, 3000-548, Coimbra, Portugal.

Submitted 15 November 2023
Resubmitted 22 July 2024
Accepted 14 January 2025
Published 5 February 2025
10.1126/scitranslmed.adm9654

Downloaded from https://www.science.org at Universita Degli Studi Di Trento on February 10, 2025